

### Supplementary Data

Protonation and formation macroconstants of  $\text{InsP}_6$

	log <i>K</i>	
	<sup>31</sup> P NMR <sup>a</sup>	Potentiometry <sup>b</sup>
$\text{L}^{12-} + \text{H}^+ \leftrightarrow \text{HL}^{11-}$	11.158(4)	10.8(1)
$\text{L}^{12-} + 2 \text{H}^+ \leftrightarrow \text{H}_2\text{L}^{10-}$	22.30(8)	21.3(1)
$\text{L}^{12-} + 3 \text{H}^+ \leftrightarrow \text{H}_3\text{L}^{9-}$	32.48(7)	31.63(6)
$\text{L}^{12-} + 4 \text{H}^+ \leftrightarrow \text{H}_4\text{L}^{8-}$	41.44(8)	40.42(6)
$\text{L}^{12-} + 5 \text{H}^+ \leftrightarrow \text{H}_5\text{L}^{7-}$	48.70(7)	47.32(6)
$\text{L}^{12-} + 6 \text{H}^+ \leftrightarrow \text{H}_6\text{L}^{6-}$	54.40(7)	53.04(7)
$\text{L}^{12-} + 7 \text{H}^+ \leftrightarrow \text{H}_7\text{L}^{5-}$	57.32(8)	56.14(9)
$\text{L}^{12-} + 8 \text{H}^+ \leftrightarrow \text{H}_8\text{L}^{4-}$	58.98(6)	58.0(1)
$\text{L}^{12-} + 9 \text{H}^+ \leftrightarrow \text{H}_9\text{L}^{3-}$	---	59.9(1)
$3 \text{Na}^+ + \text{H}_4\text{L}^{8-} \leftrightarrow [\text{Na}_3(\text{H}_4\text{L})]^{5-}$	4.80(3)	3.38(8)
$4 \text{Na}^+ + \text{H}_3\text{L}^{9-} \leftrightarrow [\text{Na}_4(\text{H}_3\text{L})]^{5-}$	6.98(3)	5.49(7)
$5 \text{Na}^+ + \text{H}_2\text{L}^{10-} \leftrightarrow [\text{Na}_5(\text{H}_2\text{L})]^{5-}$	9.25(3)	7.60(7)
$6 \text{Na}^+ + \text{L}^{12-} \leftrightarrow [\text{Na}_6\text{L}]^{6-}$	11.44(3)	9.83(8)
$3 \text{K}^+ + \text{H}_4\text{L}^{8-} \leftrightarrow [\text{K}_3(\text{H}_4\text{L})]^{5-}$	4.71(3)	3.36(5)
$4 \text{K}^+ + \text{H}_3\text{L}^{9-} \leftrightarrow [\text{K}_4(\text{H}_3\text{L})]^{5-}$	6.08(9)	5.42(5)
$5 \text{K}^+ + \text{H}_2\text{L}^{10-} \leftrightarrow [\text{K}_5(\text{H}_2\text{L})]^{5-}$	7.86(5)	7.45(5)
$6 \text{K}^+ + \text{L}^{12-} \leftrightarrow [\text{K}_6\text{L}]^{6-}$	10.12(7)	9.70(6)
$\text{Mg}^{2+} + \text{HL}^{11-} \leftrightarrow [\text{Mg}(\text{HL})]^{9-}$	5.55(4)	---
$\text{Mg}^{2+} + \text{H}_2\text{L}^{10-} \leftrightarrow [\text{Mg}(\text{H}_2\text{L})]^{8-}$	5.84(4)	6.50(8)
$\text{Mg}^{2+} + \text{H}_3\text{L}^{9-} \leftrightarrow [\text{Mg}(\text{H}_3\text{L})]^{7-}$	5.86(2)	5.34(6)
$\text{Mg}^{2+} + \text{H}_4\text{L}^{8-} \leftrightarrow [\text{Mg}(\text{H}_4\text{L})]^{6-}$	5.58(3)	3.80(6)
$\text{Mg}^{2+} + \text{H}_5\text{L}^{7-} \leftrightarrow [\text{Mg}(\text{H}_5\text{L})]^{5-}$	5.38(3)	3.24(7)
$\text{Mg}^{2+} + \text{H}_6\text{L}^{6-} \leftrightarrow [\text{Mg}(\text{H}_6\text{L})]^{4-}$	4.84(2)	2.68(6)
$5 \text{Mg}^{2+} + \text{H}_2\text{L}^{10-} \leftrightarrow [\text{Mg}_5(\text{H}_2\text{L})]$	---	21.11(5)
$\text{Ca}^{2+} + \text{L}^{12-} \leftrightarrow [\text{CaL}]^{10-}$	6.48(7)	---
$\text{Ca}^{2+} + \text{HL}^{11-} \leftrightarrow [\text{Ca}(\text{HL})]^{9-}$	6.68(7)	---
$\text{Ca}^{2+} + \text{H}_2\text{L}^{10-} \leftrightarrow [\text{Ca}(\text{H}_2\text{L})]^{8-}$	6.27(6)	6.39(3)
$\text{Ca}^{2+} + \text{H}_3\text{L}^{9-} \leftrightarrow [\text{Ca}(\text{H}_3\text{L})]^{7-}$	5.62(7)	4.86(2)
$\text{Ca}^{2+} + \text{H}_4\text{L}^{8-} \leftrightarrow [\text{Ca}(\text{H}_4\text{L})]^{6-}$	5.26(7)	3.14(7)
$\text{Ca}^{2+} + \text{H}_5\text{L}^{7-} \leftrightarrow [\text{Ca}(\text{H}_5\text{L})]^{5-}$	5.01(7)	---
$\text{Ca}^{2+} + \text{H}_6\text{L}^{6-} \leftrightarrow [\text{Ca}(\text{H}_6\text{L})]^{4-}$	4.24(5)	---

Table S1. Logarithms of the protonation and formation constants of  $\text{InsP}_6$  ( $I = 0.15 \text{ M}$ ,  $T = 37.0 \text{ }^\circ\text{C}$ ). (a) This work,  $\sigma = 0.022$  ( $\text{H}^+$ ),  $0.023$  ( $\text{Na}^+$ ),  $0.056$  ( $\text{K}^+$ ),  $0.026$  ( $\text{Mg}^{2+}$ ) and  $0.021$  ( $\text{Ca}^{2+}$ ). The uncertainties for the equilibrium constants, which are estimates of the standard deviation were calculated by HypNMR 2006 software <sup>1</sup>. (b) Potentiometric data reported previously are included for comparison<sup>2,3</sup>.

### *InsP<sub>6</sub> protonation sequence*

Table S2 lists the <sup>31</sup>P NMR individual chemical shifts and their variation while the L<sup>12-</sup> species is successively protonated ( $\Delta\delta_p$ ). All the signals are considerably affected upon protonation, being suggestive of an extensive proton sharing between the phosphate groups through hydrogen bonds. To aid in the following analysis of the spatial requirements related to the protonation sequence, Figure 4 shows the optimised 3-21+G\* geometries for both conformational states of some of the InsP<sub>6</sub> species.

$\Delta\delta_p$  values are lower for P2 and P4/P6, making highly possible for the first H<sup>+</sup> to bind to the phosphate at position 2, being shared to some extent with the phosphates at C4 or C6. According to Figures 4b and 4j, this is compatible with the 5a1e conformation of the ligand. Strikingly, the link of the second proton produces an unexpected rising of the  $\Delta\delta_p$  values, especially for P2. This phenomenon, already reported for Ins(1,4,5,6)P<sub>4</sub><sup>4-</sup>, indicates that a conformational change is operating along with the protonation reaction. Since  $\Delta\delta_p$  is similar and small for P1/P3, P4/P6 and P5, a rearrangement of the protons towards these groups is proposed, which would compensate the substantial increment of  $\delta$  brought about by the conformational change. As a result, in H<sub>2</sub>L<sup>8-</sup> the two protons could be strongly shared between P2 - P1/P3 and P4/P6 - P5 (Figures 4c and 4k).

The third incoming proton preferentially associates to P1/P3, being probably shared between neighbouring phosphate groups and affecting P2 and P4/P6 signals as well (see Table S2). As it can be seen from Figures 4d and 4l, it is likely that each of the three protons would be interchanged dynamically between a pair of phosphate groups. The formation of H<sub>4</sub>L<sup>7-</sup> is associated with a significant decrease in the chemical shift of P1/P3 and (to a lesser extent) P4/P6 signals. This fourth proton would be linked to the phosphate at C1 or C3, making the P1/P3 group to share simultaneously two H<sup>+</sup> with P4/P6 and P2 (Figures 4e and 4m). P2 signal is only slightly affected in this process, indicating that the proton at P1/P3, formerly shared to P2 in H<sub>3</sub>L<sup>9-</sup>, is shifted to P1/3 almost completely in H<sub>4</sub>L<sup>8-</sup>.

The formation of H<sub>5</sub>L<sup>7-</sup> is followed by a decrease of  $\Delta\delta_p$  for P2, P1/P3 and P5. According to the results of the molecular modelling study (Figures 4f and 4n), this is consistent with the protonation of P1/P3, and the sharing of this proton with P4/P6. In this process, P1/P3 gets away from P2, while P4/P6 gets farther from P5. This causes a rearrangement of the protons on the ligand, so that in the final state P2 retains its original proton and shares another with P1/P3, being the latter diprotonated. Besides, P4/P6 would be associated with P1/P3, moving away from P5 and explaining the negative  $\Delta\delta_p$  value for the latter. As it is expected, the sixth protonation step occurs with the filling of the only phosphate-phosphate empty space: between P4/P6 - P5, whose signals are the most affected (see Figures 4g and 4o and Table S2).

The structural analysis for the rest of the species is fairly complex. Since all the NMR signals are affected similarly, a reasonable assumption would be a continuous and dynamic rearrangement of the protons all over the ligand. In spite of that, the data in Table S2 suggest that the seventh proton could be bound mainly to P2, while the eighth would be linked to P5.

Cation	Species	Calculated chemical shifts (ppm)				$\Delta\delta_p$ (ppm)				$\Delta\delta_c$ (ppm)			
		P1/P3	P2	P4/P6	P5	P1/P3	P2	P4/P6	P5	P1/P3	P2	P4/P6	P5
H <sup>+</sup>	L <sup>12-</sup>	5.952	7.304	5.536	5.794	---	---	---	---	---	---	---	---
	HL <sup>11-</sup>	5.866	3.610	4.339	5.027	-0.086	-3.694	-1.197	-0.768	---	---	---	---
	H <sub>2</sub> L <sup>10-</sup>	6.027	4.885	4.551	5.298	0.161	1.275	0.212	0.271	---	---	---	---
	H <sub>3</sub> L <sup>9-</sup>	4.743	4.363	3.968	5.248	-1.284	-0.522	-0.583	-0.049	---	---	---	---
	H <sub>4</sub> L <sup>8-</sup>	4.074	4.395	3.908	5.293	-0.669	0.031	-0.060	0.045	---	---	---	---
	H <sub>5</sub> L <sup>7-</sup>	3.357	2.834	4.055	4.762	-0.717	-1.561	0.148	-0.531	---	---	---	---
	H <sub>6</sub> L <sup>6-</sup>	3.050	2.499	3.542	4.025	-0.307	-0.335	-0.513	-0.738	---	---	---	---
	H <sub>7</sub> L <sup>5-</sup>	2.910	2.292	3.417	4.069	-0.140	-0.207	-0.125	0.044	---	---	---	---
H <sub>8</sub> L <sup>4-</sup>	2.597	1.698	3.133	3.336	-0.313	-0.594	-0.285	-0.733	---	---	---	---	
Na <sup>+</sup>	[Na <sub>6</sub> L] <sup>6-</sup>	7.118	8.021	6.830	6.661	---	---	---	---	1.166	0.717	1.294	0.867
	[Na <sub>5</sub> (H <sub>2</sub> L)] <sup>5-</sup>	7.046	5.785	5.653	5.428	-0.072	-2.236	-1.177	-1.233	1.019	0.900	1.103	0.130
	[Na <sub>4</sub> (H <sub>3</sub> L)] <sup>5-</sup>	4.853	4.926	4.270	5.375	-2.192	-0.859	-1.384	-0.053	0.110	0.563	0.302	0.126
	[Na <sub>3</sub> (H <sub>4</sub> L)] <sup>5-</sup>	3.943	4.276	4.227	5.275	-0.910	-0.651	-0.042	-0.099	-0.131	-0.119	0.320	-0.018
K <sup>+</sup>	[K <sub>6</sub> L] <sup>6-</sup>	6.412	7.705	6.392	6.433	---	---	---	---	0.461	0.401	0.856	0.639
	[K <sub>5</sub> (H <sub>2</sub> L)] <sup>5-</sup>	6.323	4.732	5.519	5.438	-0.090	-2.973	-0.873	-0.996	0.296	-0.153	0.968	0.140
	[K <sub>4</sub> (H <sub>3</sub> L)] <sup>5-</sup>	5.784	5.144	4.416	5.344	-0.539	0.413	-1.103	-0.094	1.041	0.781	0.448	0.095
	[K <sub>3</sub> (H <sub>4</sub> L)] <sup>5-</sup>	4.072	4.484	4.159	5.345	-1.712	-0.661	-0.257	0.002	-0.002	0.089	0.251	0.052
Mg <sup>2+</sup>	[Mg(HL)] <sup>9-</sup>	5.315	7.416	5.720	5.629	---	---	---	---	-0.551	3.806	1.381	0.602
	[Mg(H <sub>2</sub> L)] <sup>8-</sup>	6.124	4.934	4.317	5.198	0.809	-2.482	-1.403	-0.431	0.097	0.049	-0.234	-0.100
	[Mg(H <sub>3</sub> L)] <sup>7-</sup>	5.158	3.089	3.902	5.246	-0.965	-1.845	-0.415	0.048	0.415	-1.274	-0.066	-0.002
	[Mg(H <sub>4</sub> L)] <sup>6-</sup>	3.934	3.297	3.534	4.817	-1.225	0.208	-0.367	-0.429	-0.141	-1.097	-0.373	-0.476
	[Mg(H <sub>5</sub> L)] <sup>5-</sup>	3.063	2.453	3.593	4.291	-0.870	-0.844	0.059	-0.526	-0.294	-0.380	-0.463	-0.471
	[Mg(H <sub>6</sub> L)] <sup>4-</sup>	2.751	2.105	3.262	3.800	-0.313	-0.349	-0.331	-0.492	-0.299	-0.394	-0.280	-0.225
Ca <sup>2+</sup>	[CaL] <sup>10-</sup>	6.133	7.530	6.139	5.931	---	---	---	---	0.181	0.226	0.603	0.137
	[Ca(HL)] <sup>9-</sup>	6.033	7.479	3.952	6.610	-0.099	-0.051	-2.187	0.679	0.167	3.869	-0.387	1.584
	[Ca(H <sub>2</sub> L)] <sup>8-</sup>	6.348	3.344	4.338	3.995	0.315	-4.135	0.385	-2.616	0.321	-1.541	-0.213	-1.303
	[Ca(H <sub>3</sub> L)] <sup>7-</sup>	5.276	4.630	4.167	5.029	-1.072	1.286	-0.171	1.035	0.533	0.267	0.199	-0.219
	[Ca(H <sub>4</sub> L)] <sup>6-</sup>	4.282	3.562	4.025	4.786	-0.994	-1.068	-0.141	-0.243	0.208	-0.833	0.118	-0.507
	[Ca(H <sub>5</sub> L)] <sup>5-</sup>	3.294	2.507	3.701	4.347	-0.988	-1.054	-0.324	-0.439	-0.063	-0.326	-0.354	-0.415
	[Ca(H <sub>6</sub> L)] <sup>4-</sup>	2.715	2.053	3.197	3.708	-0.580	-0.455	-0.504	-0.639	-0.335	-0.446	-0.345	-0.317

Table S2. Calculated <sup>31</sup>P NMR chemical shifts (HypNMR software <sup>1</sup>) for InsP<sub>6</sub> in the absence and presence of M<sup>+</sup> or M<sup>2+</sup> (*I* = 0.15 M, *T* = 37.0 °C). The change in the chemical shifts due only to the protonation ( $\Delta\delta_p$ ) or complexation ( $\Delta\delta_c$ ) processes are included.

### Application of the Cluster Expansion Method

The NMR data were analyzed by the Cluster Expansion Method <sup>5</sup>. Starting from the macrostates  $L^{12-}$ ,  $HL^{11-}$ ,  $H_2L^{10-}$ ,  $H_3L^{9-}$ ,  $H_4L^{8-}$ ,  $H_5L^{7-}$  and  $H_6L^{6-}$ , we can construct 64 microstates depending on the particular pattern of protonation of the phosphate groups. These different microstates are specified by introducing a two-valued state variable  $S_i$  for each individual site  $i$ , such that  $S_i = 1$  if the site is protonated and  $S_i = 0$  if the site is deprotonated. Hence, the 64 possible microstates are: {0,0,0,0,0,0}, {1,0,0,0,0,0}, {0,0,1,0,0,0}, {0,1,0,0,0,0}, {0,0,0,1,0,0}, {0,0,0,0,1,0}, {1,1,0,0,0,0}, {0,1,1,0,0,0}, {1,0,0,1,0,0}, {0,0,1,0,0,1}, {1,0,0,0,1,0}, {0,0,1,0,1,0}, {1,0,0,0,0,1}, {0,0,1,1,0,0}, {1,0,1,0,0,0}, {0,1,0,1,0,0}, {0,1,0,0,0,1}, {0,1,0,0,1,0}, {0,0,0,1,1,0}, {0,0,0,0,1,1}, {0,0,0,1,0,1}, {1,1,1,0,0,0}, {1,1,0,1,0,0}, {0,1,1,0,0,1}, {1,1,0,0,1,0}, {0,1,1,0,1,0}, {1,0,1,1,0,0}, {1,0,1,0,0,1}, {1,0,1,0,1,0}, {1,0,0,1,1,0}, {0,0,1,1,1,0}, {1,0,0,0,1,1}, {0,0,1,1,0,1}, {1,0,0,1,0,1}, {0,1,0,1,0,1}, {0,1,0,1,1,0}, {0,1,0,0,1,1}, {0,0,0,1,1,1}, {1,1,1,1,0,0}, {1,1,1,0,0,1}, {1,1,0,1,1,0}, {0,1,1,0,1,1}, {1,0,1,1,1,0}, {1,0,1,0,1,1}, {1,0,1,1,0,1}, {1,0,0,1,1,1}, {0,0,1,1,1,1}, {1,1,1,0,1,0}, {0,1,1,1,1,0}, {1,1,0,0,1,1}, {0,1,0,1,1,1}, {0,1,1,1,0,1}, {1,1,0,1,0,1}, {0,1,1,1,1,1}, {1,1,0,1,1,1}, {1,1,1,1,0,1}, {1,1,1,1,1,0}, {1,1,1,1,1,1}, {1,1,1,1,1,1}.

Taking into account the symmetry of the system under consideration, the cluster expansion model applied was:

$$\begin{aligned} \delta_{1/3} &= \delta_{1/3}^{(0)} + \left( \frac{1}{1 + \beta_1 10^{-pH} + \beta_2 10^{-2pH} + \beta_3 10^{-3pH} + \beta_4 10^{-4pH} + \beta_5 10^{-5pH} + \beta_6 10^{-6pH}} \right) \left( \frac{A(\beta_1 10^{-pH}) + B(\beta_4 10^{-4pH})}{D(\beta_4 10^{-4pH}) + E(\beta_1 10^{-pH})} \right) \end{aligned} \quad (1)$$

$$\delta_2 = \delta_2^{(0)} + \left( \frac{1}{1 + \beta_1 10^{-pH} + \beta_2 10^{-2pH} + \beta_3 10^{-3pH} + \beta_4 10^{-4pH} + \beta_5 10^{-5pH} + \beta_6 10^{-6pH}} \right) \left( \frac{G(\beta_1 10^{-pH}) + H(\beta_4 10^{-4pH})}{J(\beta_4 10^{-4pH}) + K(\beta_1 10^{-pH})} \right) \quad (2)$$

$$\delta_{4/6} = \delta_{4/6}^{(0)} + \left( \frac{1}{1 + \beta_1 10^{-pH} + \beta_2 10^{-2pH} + \beta_3 10^{-3pH} + \beta_4 10^{-4pH} + \beta_5 10^{-5pH} + \beta_6 10^{-6pH}} \right) \left( \frac{M(\beta_1 10^{-pH}) + N(\beta_4 10^{-4pH})}{P(\beta_4 10^{-4pH}) + Q(\beta_1 10^{-pH})} \right) \quad (3)$$

$$\delta_5 = \delta_5^{(0)} + \left( \frac{1}{1 + \beta_1 10^{-pH} + \beta_2 10^{-2pH} + \beta_3 10^{-3pH} + \beta_4 10^{-4pH} + \beta_5 10^{-5pH} + \beta_6 10^{-6pH}} \right) \left( \frac{S(\beta_1 10^{-pH}) + T(\beta_4 10^{-4pH})}{V(\beta_4 10^{-4pH}) + W(\beta_1 10^{-pH})} \right) \quad (4)$$

where  $\delta_{1/3}^{(0)}$ ,  $\delta_2^{(0)}$ ,  $\delta_{4/6}^{(0)}$  and  $\delta_5^{(0)}$  are the chemical shifts for P1 (or P3), P2, P4 (or P6) and P5 respectively, when all groups are deprotonated,  $\beta_1$ ,  $\beta_2$ ,  $\beta_3$ ,  $\beta_4$ ,  $\beta_5$  and  $\beta_6$  are the logarithms of the

overall protonation constants, and A, B, C, D, E, F, G, H, I, J, K, L, M, N, O, P, Q, R, S, T, U, V, W and X are defined as:

$$A = (\Delta_{11} + \Delta_{13})\pi(\{1,0,0,0,0,0\}) + (\Delta_{12})\pi(\{0,1,0,0,0,0\}) + (\Delta_{14} + \Delta_{16})\pi(\{0,0,0,1,0,0\}) + \Delta_{15}(1 - 2\pi(\{1,0,0,0,0,0\}) - 2\pi(\{0,0,0,1,0,0\}) - \pi(\{0,1,0,0,0,0\}))$$

(5)

$$B = (\Delta_{11} + \Delta_{13})(\pi(\{1,1,0,0,0,0\}) + \pi(\{1,0,0,1,0,0\}) + \pi(\{1,0,0,0,1,0\}) + \pi(\{1,0,0,0,0,1\})) + (\Delta_{12})(2\pi(\{1,1,0,0,0,0\}) + 2\pi(\{0,1,0,1,0,0\}) + \pi(\{0,1,0,0,1,0\})) + (\Delta_{16} + \Delta_{14})(\pi(\{1,0,0,1,0,0\}) + \pi(\{0,1,0,1,0,0\}) + \pi(\{1,0,0,0,0,1\}) + \pi(\{0,0,0,1,1,0\}) + \pi(\{0,0,0,1,0,1\})) + (\Delta_{15})(2\pi(\{1,0,0,0,1,0\}) + 2\pi(\{0,0,0,1,1,0\}) + \pi(\{0,1,0,0,1,0\}))$$

(6)

$$C = (\Delta_{11} + \Delta_{13})\left(\pi(\{1,1,1,0,0,0\}) + \pi(\{1,1,0,1,0,0\}) + \pi(\{1,1,0,0,1,0\}) + \pi(\{1,0,1,0,1,0\}) + \pi(\{1,0,0,1,1,0\}) + \pi(\{0,1,1,1,0,0\}) + \pi(\{0,0,1,1,1,0\}) + \pi(\{0,0,1,1,0,1\}) + \pi(\{0,0,1,1,0,1\})\right) + (\Delta_{12})\left(\pi(\{1,1,1,0,0,0\}) + 2\pi(\{0,1,1,1,0,0\}) + 2\pi(\{1,1,0,0,1,0\}) + 2\pi(\{1,1,0,0,1,0\}) + 2\pi(\{0,1,1,0,1,0\}) + 2\pi(\{0,1,0,1,1,0\}) + \pi(\{0,1,0,1,0,1\})\right) + (\Delta_{16} + \Delta_{14})\left(\pi(\{0,1,1,1,0,0\}) + \pi(\{1,0,1,1,0,0\}) + \pi(\{1,1,0,1,0,0\}) + \pi(\{0,1,0,1,1,0\}) + \pi(\{0,1,0,1,0,1\}) + \pi(\{0,0,1,1,1,0\}) + 2\pi(\{0,0,1,1,0,1\}) + \pi(\{1,0,0,1,1,0\}) + \pi(\{0,0,1,1,0,1\}) + \pi(\{0,0,1,1,1,0\}) + \pi(\{0,0,1,1,1,0\}) + \pi(\{0,0,0,1,1,1\}) + \pi(\{0,0,0,1,1,1\})\right) + (\Delta_{15})\left(2\pi(\{1,1,0,0,1,0\}) + \pi(\{1,0,1,0,1,0\}) + 2\pi(\{1,0,0,1,1,0\}) + 2\pi(\{0,0,1,1,1,0\}) + 2\pi(\{0,1,0,1,1,0\}) + \pi(\{0,0,0,1,1,1\})\right)$$

(7)

$$D = (\Delta_{11} + \Delta_{13})\left(2\pi(\{1,1,1,1,0,0\}) + \pi(\{1,1,1,0,1,0\}) + \pi(\{1,1,0,1,1,0\}) + 2\pi(\{1,0,1,1,1,0\}) + \pi(\{1,0,1,1,0,1\}) + \pi(\{1,0,0,1,1,1\}) + \pi(\{0,1,1,1,1,0\}) + \pi(\{0,1,1,1,0,1\})\right) + (\Delta_{12})\left(2\pi(\{1,1,1,1,0,0\}) + \pi(\{1,1,1,0,1,0\}) + 2\pi(\{1,1,0,1,1,0\}) + 2\pi(\{0,1,1,1,1,0\}) + 2\pi(\{0,1,1,1,0,1\}) + \pi(\{0,1,0,1,1,1\})\right) + (\Delta_{16} + \Delta_{14})\left(\pi(\{1,1,1,1,0,0\}) + \pi(\{1,1,0,1,1,0\}) + \pi(\{1,0,1,1,1,0\}) + \pi(\{1,0,1,1,0,1\}) + \pi(\{0,1,1,1,1,0\}) + \pi(\{0,1,1,1,0,1\}) + \pi(\{0,1,1,1,1,1\}) + \pi(\{0,1,1,1,1,1\})\right) + (\Delta_{15})\left(\pi(\{1,1,1,0,1,0\}) + 2\pi(\{1,0,1,1,1,0\}) + 2\pi(\{1,0,0,1,1,1\}) + 2\pi(\{1,1,0,1,1,0\}) + 2\pi(\{0,1,1,1,1,0\}) + \pi(\{0,1,0,1,1,1\})\right)$$

(8)

$$E = (\Delta_{11} + \Delta_{13})(1 - \pi(\{1,1,0,1,1,1\})) + (\Delta_{12})\left(2\pi(\{1,1,1,1,1,0\}) + \pi(\{1,1,1,1,0,1\})\right) +$$

$$+ (\Delta_{16} + \Delta_{14})(1 - \pi(\{1,1,1,1,0\})) + (\Delta_{15})(1 - \pi(\{1,1,1,0,1\}))$$

(9)

$$F = \Delta_{11} + \Delta_{12} + \Delta_{13} + \Delta_{14} + \Delta_{15} + \Delta_{16}$$

(10)

$$G = (2\Delta_{21})\pi(\{1,0,0,0,0\}) + (\Delta_{22})\pi(\{0,1,0,0,0\}) + (2\Delta_{24})\pi(\{0,0,0,1,0\}) + \\ + \Delta_{25}(1 - 2\pi(\{1,0,0,0,0\}) - 2\pi(\{0,0,0,1,0\}) - \pi(\{0,1,0,0,0\}))$$

(11)

$$H = (2\Delta_{21})(\pi(\{1,1,0,0,0\}) + \pi(\{1,0,0,1,0\}) + \pi(\{1,0,0,0,1\}) + \pi(\{1,0,0,0,0\})) + \\ + (\Delta_{22})(2\pi(\{1,1,0,0,0\}) + 2\pi(\{0,1,0,1,0\}) + \pi(\{0,1,0,0,1\})) + \\ (2\Delta_{24})\left(\frac{\pi(\{1,0,0,1,0\}) + \pi(\{0,1,0,1,0\}) + \pi(\{1,0,0,0,1\})}{\pi(\{0,0,0,1,1\}) + \pi(\{0,0,0,1,0\})} + \right) + \\ + (\Delta_{25})\left(\frac{2\pi(\{1,0,0,0,1,0\}) + 2\pi(\{0,0,0,1,1,0\})}{\pi(\{0,1,0,0,1,0\})} + \right)$$

(12)

$$I = (2\Delta_{21})\left(\frac{\pi(\{1,1,1,0,0\}) + \pi(\{1,1,0,1,0\}) + \pi(\{1,1,0,0,1\}) + 2\pi(\{1,1,0,0,0\})}{\pi(\{1,0,1,0,1\}) + \pi(\{1,0,0,1,1\}) + \pi(\{0,1,1,1,0\}) + \pi(\{0,0,1,1,1\})} + \right) + \\ + (\Delta_{22})\left(\frac{\pi(\{1,1,1,0,0\}) + 2\pi(\{0,1,1,1,0\}) + 2\pi(\{1,1,0,0,1,0\})}{2\pi(\{1,1,0,1,0\}) + 2\pi(\{0,1,0,1,1,0\}) + \pi(\{0,1,0,1,0,1\})} + \right) + \\ + (2\Delta_{24})\left(\frac{\pi(\{0,1,1,1,0,0\}) + \pi(\{1,0,1,1,0,0\}) + \pi(\{1,1,0,1,0,0\}) + \pi(\{0,1,0,1,1,0\}) + \pi(\{0,0,1,1,1,0\})}{\pi(\{0,0,1,1,1,0\}) + 2\pi(\{0,0,1,1,0,1\}) + \pi(\{1,0,0,1,1,0\}) + \pi(\{0,0,0,1,1,1\})} + \right) + \\ + (\Delta_{25})\left(\frac{2\pi(\{1,1,0,0,1,0\}) + \pi(\{1,0,1,0,1,0\}) + 2\pi(\{1,0,0,1,1,0\})}{2\pi(\{0,0,1,1,1,0\}) + 2\pi(\{0,1,0,1,1,0\}) + \pi(\{0,0,0,1,1,1\})} + \right)$$

(13)

$$J = (2\Delta_{21})\left(\frac{2\pi(\{1,1,1,1,0,0\}) + \pi(\{1,1,1,0,1,0\}) + \pi(\{1,1,0,1,1,0\}) + 2\pi(\{1,0,1,1,1,0\})}{\pi(\{1,0,1,1,0,1\}) + \pi(\{1,0,0,1,1,1\}) + \pi(\{0,1,1,1,1,0\}) + \pi(\{0,1,1,1,0,1\})} + \right) + \\ + (\Delta_{22})\left(\frac{2\pi(\{1,1,1,1,0,0\}) + \pi(\{1,1,1,0,1,0\}) + 2\pi(\{1,1,0,1,1,0\})}{2\pi(\{0,1,1,1,1,0\}) + 2\pi(\{0,1,1,1,0,1\}) + \pi(\{0,1,0,1,1,1\})} + \right) + \\ + (2\Delta_{24})\left(\frac{\pi(\{1,1,1,1,0,0\}) + \pi(\{1,1,0,1,1,0\}) + \pi(\{1,0,1,1,1,0\}) + \pi(\{1,0,1,1,0,1\})}{2\pi(\{1,0,0,1,1,1\}) + \pi(\{0,1,1,1,1,0\}) + 2\pi(\{0,1,1,1,0,1\}) + \pi(\{0,1,0,1,1,1\})} + \right) + \\ + (\Delta_{25})\left(\frac{\pi(\{1,1,1,0,1,0\}) + 2\pi(\{1,0,1,1,1,0\}) + 2\pi(\{1,0,0,1,1,1\})}{2\pi(\{1,1,0,1,1,0\}) + 2\pi(\{0,1,1,1,1,0\}) + \pi(\{0,1,0,1,1,1\})} + \right)$$

(14)

$$K = (2\Delta_{21})(1 - \pi(\{1,1,0,1,1,1\})) + (\Delta_{22})\left(\frac{2\pi(\{1,1,1,1,1,0\}) + 2\pi(\{1,1,0,1,1,1\})}{\pi(\{1,1,1,1,0,1\})} + \right)$$

$$+ (2\Delta_{24})(1 - \pi(\{1,1,1,1,0\})) + (\Delta_{25})(1 - \pi(\{1,1,1,0,1\}))$$

(15)

$$L = 2\Delta_{21} + \Delta_{22} + 2\Delta_{24} + \Delta_{25}$$

(16)

$$M = (\Delta_{41} + \Delta_{43})\pi(\{1,0,0,0,0\}) + (\Delta_{42})\pi(\{0,1,0,0,0\}) + (\Delta_{44} + \Delta_{46})\pi(\{0,0,0,1,0\}) + \\ + \Delta_{45}(1 - 2\pi(\{1,0,0,0,0\}) - 2\pi(\{0,0,0,1,0\}) - \pi(\{0,1,0,0,0\}))$$

(17)

$$N = (\Delta_{41} + \Delta_{43})\left(\frac{\pi(\{1,1,0,0,0\}) + \pi(\{1,0,0,1,0\}) + \pi(\{1,0,0,0,1\})}{\pi(\{1,0,0,0,1\}) + \pi(\{1,0,1,0,0\})}\right) + \\ + (\Delta_{42})(2\pi(\{1,1,0,0,0\}) + 2\pi(\{0,1,0,1,0\}) + \pi(\{0,1,0,0,1\})) + \\ + (\Delta_{46} + \Delta_{44})\left(\frac{\pi(\{1,0,0,1,0\}) + \pi(\{0,1,0,1,0\}) + \pi(\{1,0,0,0,1\})}{\pi(\{0,0,0,1,1\}) + \pi(\{0,0,0,1,0\})}\right) + \\ + (\Delta_{45})(2\pi(\{1,0,0,0,1\}) + 2\pi(\{0,0,0,1,1\}) + \pi(\{0,1,0,0,1\}))$$

(18)

O

$$= (\Delta_{41} + \Delta_{43})\left(\frac{\pi(\{1,1,1,0,0\}) + \pi(\{1,1,0,1,0\}) + \pi(\{1,1,0,0,1\}) + 2\pi(\{1,0,0,1,1\})}{\pi(\{1,0,0,1,1\}) + \pi(\{0,1,1,1,0\}) + \pi(\{0,0,1,1,1\})}\right) + \\ + (\Delta_{42})\left(\frac{\pi(\{1,1,1,0,0\}) + 2\pi(\{0,1,1,1,0\}) + 2\pi(\{1,1,0,0,1\})}{2\pi(\{1,1,0,1,0\}) + 2\pi(\{0,1,0,1,1\}) + \pi(\{0,1,0,1,1\})}\right) + \\ + (\Delta_{46} + \Delta_{44})\left(\frac{\pi(\{0,1,1,1,0\}) + \pi(\{1,0,1,1,0\}) + \pi(\{1,1,0,1,0\}) + \pi(\{0,1,0,1,1\}) + \pi(\{0,0,0,1,1\})}{\pi(\{0,0,1,1,1\}) + 2\pi(\{0,0,1,1,0\}) + \pi(\{1,0,0,1,1\}) + \pi(\{0,0,0,1,1\})}\right) + \\ + (\Delta_{45})\left(\frac{2\pi(\{1,1,0,0,1\}) + \pi(\{1,0,1,0,1\}) + 2\pi(\{1,0,0,1,1\})}{2\pi(\{0,0,1,1,1\}) + 2\pi(\{0,1,0,1,1\}) + \pi(\{0,0,0,1,1\})}\right)$$

(19)

$$P = (\Delta_{41} + \Delta_{43})\left(\frac{2\pi(\{1,1,1,1,0\}) + \pi(\{1,1,1,0,1\}) + \pi(\{1,1,0,1,1\}) + 2\pi(\{1,0,1,1,0\})}{\pi(\{1,0,1,1,0\}) + \pi(\{1,0,0,1,1\}) + \pi(\{0,1,1,1,0\}) + \pi(\{0,1,1,1,0\})}\right) + \\ + (\Delta_{42})\left(\frac{2\pi(\{1,1,1,1,0\}) + \pi(\{1,1,1,0,1\}) + 2\pi(\{1,1,0,1,1\})}{2\pi(\{0,1,1,1,0\}) + 2\pi(\{0,1,1,1,0\}) + \pi(\{0,1,0,1,1\})}\right) + \\ + (\Delta_{46} + \Delta_{44})\left(\frac{\pi(\{1,1,1,1,0\}) + \pi(\{1,1,0,1,1\}) + \pi(\{1,0,1,1,0\}) + \pi(\{1,0,1,1,0\})}{2\pi(\{1,0,0,1,1\}) + \pi(\{0,1,1,1,0\}) + 2\pi(\{0,1,1,1,0\}) + \pi(\{0,1,0,1,1\})}\right) + \\ + (\Delta_{45})\left(\frac{\pi(\{1,1,1,0,1\}) + 2\pi(\{1,0,1,1,0\}) + 2\pi(\{1,0,0,1,1\})}{2\pi(\{1,1,0,1,1\}) + 2\pi(\{0,1,1,1,0\}) + \pi(\{0,1,0,1,1\})}\right)$$

(20)

Q

$$= (\Delta_{41} + \Delta_{43})(1 - \pi(\{1,1,0,1,1\})) + (\Delta_{42})(2\pi(\{1,1,1,1,0\}) + 2\pi(\{1,1,0,1,1\}))$$

$$+ (\Delta_{46} + \Delta_{44})(1 - \pi(\{1,1,1,1,1,0\})) + (\Delta_{45})(1 - \pi(\{1,1,1,1,0,1\}))$$

(21)

$$R = \Delta_{41} + \Delta_{42} + \Delta_{43} + \Delta_{44} + \Delta_{45} + \Delta_{46}$$

(22)

$$S = (2\Delta_{51})\pi(\{1,0,0,0,0,0\}) + (\Delta_{52})\pi(\{0,1,0,0,0,0\}) + (2\Delta_{54})\pi(\{0,0,0,1,0,0\}) + \\ + \Delta_{55}(1 - 2\pi(\{1,0,0,0,0,0\}) - 2\pi(\{0,0,0,1,0,0\}) - \pi(\{0,1,0,0,0,0\}))$$

(23)

$$T = (2\Delta_{51})(\pi(\{1,1,0,0,0,0\}) + \pi(\{1,0,0,1,0,0\}) + \pi(\{1,0,0,0,1,0\}) + \pi(\{1,0,0,0,0,1\})) + \\ + (\Delta_{52})(2\pi(\{1,1,0,0,0,0\}) + 2\pi(\{0,1,0,1,0,0\}) + \pi(\{0,1,0,0,1,0\})) + \\ + (2\Delta_{54})(\pi(\{1,0,0,1,0,0\}) + \pi(\{0,1,0,1,0,0\}) + \pi(\{1,0,0,0,0,1\}) + \pi(\{0,0,0,1,1,0\}) + \pi(\{0,0,0,1,0,1\})) + \\ + (\Delta_{55})(2\pi(\{1,0,0,0,1,0\}) + 2\pi(\{0,0,0,1,1,0\}) + \pi(\{0,1,0,0,1,0\}))$$

(24)

$$U = (2\Delta_{51})\left(\pi(\{1,1,1,0,0,0\}) + \pi(\{1,1,0,1,0,0\}) + \pi(\{1,1,0,0,1,0\}) + 2\pi(\{1,0,1,1,0,0\}) + \pi(\{1,0,0,1,1,0\}) + \pi(\{0,1,1,1,0,0\}) + \pi(\{0,0,1,1,1,0\}) + \pi(\{0,0,1,1,0,1\})\right) + \\ + (\Delta_{52})\left(\pi(\{1,1,1,0,0,0\}) + 2\pi(\{0,1,1,1,0,0\}) + 2\pi(\{1,1,0,0,1,0\}) + 2\pi(\{1,1,0,0,0,1\}) + 2\pi(\{1,1,0,1,0,0\}) + 2\pi(\{0,1,0,1,1,0\}) + \pi(\{0,1,0,1,0,1\})\right) + \\ + (2\Delta_{54})\left(\pi(\{0,1,1,1,0,0\}) + \pi(\{1,0,1,1,0,0\}) + \pi(\{1,1,0,1,0,0\}) + \pi(\{0,1,0,1,1,0\}) + \pi(\{0,1,0,1,0,1\}) + \pi(\{0,0,1,1,1,0\}) + 2\pi(\{0,0,1,1,0,1\}) + \pi(\{1,0,0,1,1,0\}) + \pi(\{0,0,0,1,1,1\})\right) + \\ + (\Delta_{55})\left(2\pi(\{1,1,0,0,1,0\}) + \pi(\{1,0,1,0,1,0\}) + 2\pi(\{1,0,0,1,1,0\}) + 2\pi(\{0,0,1,1,1,0\}) + 2\pi(\{0,1,0,1,1,0\}) + \pi(\{0,0,0,1,1,1\})\right)$$

(25)

$$V = (2\Delta_{51})\left(2\pi(\{1,1,1,1,0,0\}) + \pi(\{1,1,1,0,1,0\}) + \pi(\{1,1,0,1,1,0\}) + 2\pi(\{1,0,1,1,1,0\}) + \pi(\{1,0,1,1,0,1\}) + \pi(\{1,0,0,1,1,1\}) + \pi(\{0,1,1,1,1,0\}) + \pi(\{0,1,1,1,0,1\})\right) + \\ + (\Delta_{52})\left(2\pi(\{1,1,1,1,0,0\}) + \pi(\{1,1,1,0,1,0\}) + 2\pi(\{1,1,0,1,1,0\}) + 2\pi(\{1,1,0,0,1,1\}) + 2\pi(\{1,1,0,1,0,1\}) + 2\pi(\{0,1,1,1,1,0\}) + \pi(\{0,1,0,1,1,1\})\right) + \\ + (2\Delta_{54})\left(\pi(\{1,1,1,1,0,0\}) + \pi(\{1,1,0,1,1,0\}) + \pi(\{1,0,1,1,1,0\}) + \pi(\{1,0,1,1,0,1\}) + \pi(\{1,0,1,1,0,1\}) + \pi(\{1,0,0,1,1,1\}) + \pi(\{0,1,1,1,1,0\}) + 2\pi(\{0,1,1,1,0,1\}) + \pi(\{0,1,0,1,1,1\})\right) + \\ + (\Delta_{55})\left(\pi(\{1,1,1,0,1,0\}) + 2\pi(\{1,0,1,1,1,0\}) + 2\pi(\{1,0,0,1,1,1\}) + 2\pi(\{1,1,0,0,1,1\}) + 2\pi(\{1,1,0,0,0,1\}) + 2\pi(\{0,1,1,1,1,0\}) + \pi(\{0,1,0,1,1,1\})\right)$$

(26)

$$W = (2\Delta_{51})(1 - \pi(\{1,1,0,1,1,1\})) + (\Delta_{52})(2\pi(\{1,1,1,1,1,0\}) + 2\pi(\{1,1,0,1,1,1\}) + \pi(\{1,1,1,1,0,1\})) + \\ + (2\Delta_{54})(1 - \pi(\{1,1,1,1,1,0\})) + (\Delta_{55})(1 - \pi(\{1,1,1,1,0,1\}))$$

(27)

$$X = 2\Delta_{51} + \Delta_{52} + 2\Delta_{54} + \Delta_{55}$$

(28)

The cluster parameters  $\Delta_{im}$  are the chemical shift increment representing the change in the chemical shift of a phosphorus nucleus *i*, while a given site *m* changes its state from deprotonated to protonated, and  $\pi(\{S_{ij}\})$  is the conditional probability of finding a particular microstate within its macrostate. A nonlinear regression was performed, fitting the experimental points to the Eqs. (1), (2), (3) and (4). Then, starting from the values obtained for A–X, the equation system (5)–(28) was solved, setting the inputs from the data previously reported for  $\text{Ins}(1,2,3)P_3$ <sup>6</sup> and  $\text{Ins}(1,3,4,5,6)P_5$ <sup>7</sup>, and with the sole restriction that the  $\pi(\{S_{ij}\})$  must take values between 0 and 1. The obtained results are depicted in Table S3.

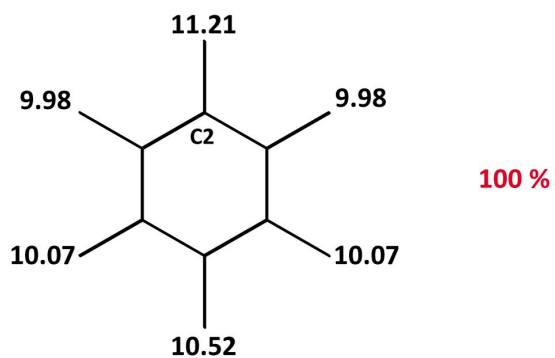
Cluster parameters		Microprotonation constants											
		<i>i</i>	log $k_i$	<i>p<sub>i</sub></i>	log $k_{p_i}$	<i>ppi</i>	log $k_{ppi}$	<i>pppi</i>	log $k_{pppi}$	<i>ppppi</i>	log $k_{ppppi}$	<i>pppppi</i>	log $k_{pppppi}$
$\Delta_{11}$	-3.158	1/3	9.98	13/31	10.76	123/321	10.62	1234/1236	8.87	12346/12364	7.61	124563/326541	10.15
$\Delta_{12}$	-0.087	2	11.21	12/32	11.07	124/326	9.37	1235	8.50	12345/12365	7.29	123456/321654	6.40
$\Delta_{13}$	-0.156	4/6	10.07	14/36	11.20	125/325	9.60	1243/3261	10.12	12354/12356	9.29	123465	6.08
$\Delta_{14}$	0.608	5	10.52	15/35	9.42	126/324	7.74	1245/3265	8.39	12453/32651	9.02	134562	7.45
$\Delta_{15}$	-0.696			16/34	11.20	142/362	9.24	1246/3264	6.48	12456/32564	5.27		
$\Delta_{16}$	0.608			21/23	9.84	143/361	10.26	1253/3251	9.52	13452/13652	9.28		
$\Delta_{21}$	-0.136			24/26	8.24	145/365	8.21	1254/3256	8.16	13456/13654	8.23		
$\Delta_{22}$	-3.747			25	10.70	146/364	8.31	1256/3254	6.53	13462	7.27		
$\Delta_{24}$	-0.283			41/63	11.10	152/352	11.25	1342/3162	9.10	13465	5.90		
$\Delta_{25}$	-0.303			42/62	12.34	153/351	9.66	1345/3165	7.11	14562/36542	7.59		
$\Delta_{41}$	0.178			43/61	9.48	154/356	9.99	1346/3164	9.44	14563/36541	10.29		
$\Delta_{42}$	-1.167			45/65	9.31	156/354	8.36	1352	11.11	23451/21653	10.65		
$\Delta_{43}$	0.178			46/64	8.81	162/342	9.24	1354/1356	9.49	23456/21654	6.90		
$\Delta_{44}$	-2.334			51/53	8.88	163/341	11.89	1452/1652	9.42	23461/21643	11.25		
$\Delta_{45}$	0.644			52	11.39	164/346	9.94	1453/1651	9.16	23465/21645	7.18		
$\Delta_{46}$	0.667			54/56	8.86	165/345	8.21	1456/1654	7.10	24561/24563	9.37		
$\Delta_{51}$	-0.276					132	10.93	2341/2163	11.75				
$\Delta_{52}$	-0.741					134/136	10.70	2345/2165	8.39				

$\Delta_{54}$	0.374					135	8.10	2346/2164	8.11				
$\Delta_{55}$	-1.087					241/263	10.97	3451/1653	10.79				
						243/261	9.34	3452/1652	9.42				
$\pi(\{1,0,0,0,0,0\})$	0.000					245/265	9.49	3456/1654	8.73				
$\pi(\{0,1,0,0,0,0\})$	1.000					246/264	6.98	3461/1643	11.39				
$\pi(\{0,0,0,1,0,0\})$	0.000					251/253	8.74	3462/1642	7.41				
$\pi(\{0,0,1,0,0,0\})$	0.000					254/256	7.03	3465/1645	7.00				
$\pi(\{1,1,0,0,0,0\})$	0.000					451/653	10.01	2451/2653	9.87				
$\pi(\{1,0,0,1,0,0\})$	0.033					452/652	9.56	2453/2651	8.24				
$\pi(\{1,0,0,0,1,0\})$	0.000					453/651	8.38	2456/2654	5.77				
$\pi(\{1,0,0,0,0,1\})$	0.006					456/654	7.60	2461/2463	8.84				
$\pi(\{1,0,1,0,0,0\})$	0.000					461/463	10.61	2465	8.28				
$\pi(\{0,1,0,1,0,0\})$	0.027					462	7.55	4561/4563	9.51				
$\pi(\{0,1,0,0,1,0\})$	0.470					465	8.10	4562	7.73				
$\pi(\{0,0,0,1,1,0\})$	0.000												
$\pi(\{0,0,0,1,0,1\})$	0.400												
$\pi(\{1,1,1,0,0,0\})$	0.194												
$\pi(\{1,1,0,1,0,0\})$	0.000												
$\pi(\{1,1,0,0,1,0\})$	0.000												
$\pi(\{1,0,1,1,0,0\})$	0.115												
$\pi(\{1,0,1,0,1,0\})$	0.110												
$\pi(\{1,0,0,1,1,0\})$	0.000												
$\pi(\{0,1,1,1,0,0\})$	0.000												
$\pi(\{0,0,1,1,1,0\})$	0.000												
$\pi(\{0,0,1,1,0,1\})$	0.000												
$\pi(\{0,1,0,1,1,0\})$	0.000												
$\pi(\{0,1,0,1,0,1\})$	0.466												
$\pi(\{0,0,0,1,1,1\})$	0.000												
$\pi(\{1,1,1,1,0,0\})$	0.194												
$\pi(\{1,1,1,0,1,0\})$	0.000												
$\pi(\{1,1,0,1,1,0\})$	0.000												
$\pi(\{1,0,1,1,1,0\})$	0.000												
$\pi(\{1,0,1,1,0,1\})$	0.417												
$\pi(\{1,0,0,1,1,1\})$	0.000												
$\pi(\{0,1,1,1,1,0\})$	0.000												
$\pi(\{0,1,1,1,0,1\})$	0.000												

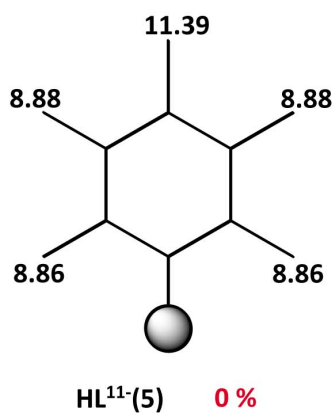
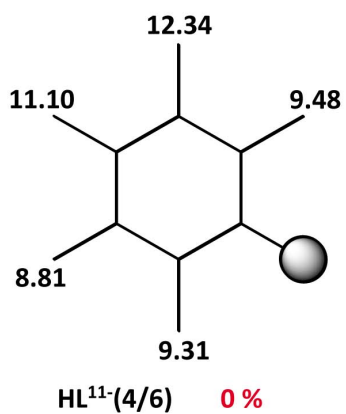
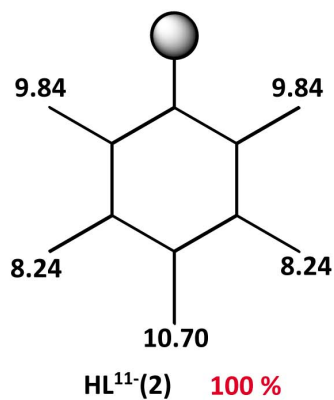
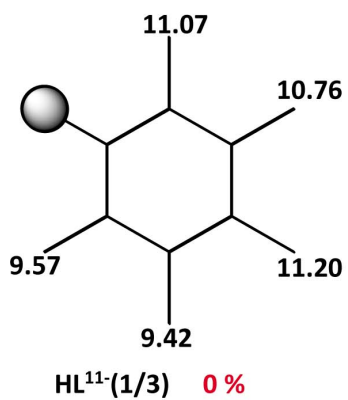
$\pi(\{0,1,0,1,1,1\})$	0.194												
$\pi(\{1,1,0,1,1,1\})$	0.057												
$\pi(\{1,1,1,1,1,0\})$	0.197												
$\pi(\{1,1,1,1,0,1\})$	0.423												
$\pi(\{1,0,1,1,1,1\})$	0.071												

Table S3. Adjusted values of the cluster expansion parameters,  $\Delta_{lm}$  and  $\pi(\{S\})$ , and logarithms of the microprotonation constants ( $k$ ) for  $\text{InsP}_6$  in  $\text{NMe}_4\text{Cl}$  0.15 M at 37.0 °C. The subscript  $i$  represents the phosphate site being protonated while  $p$  denotes the sites already protonated.

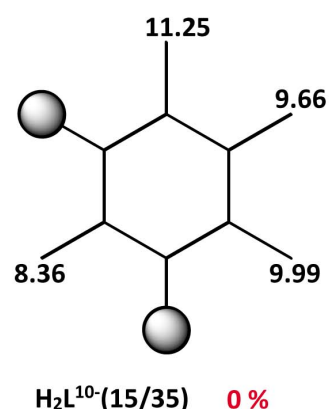
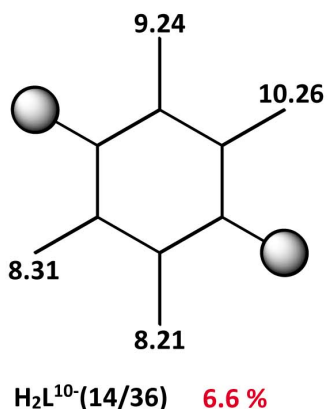
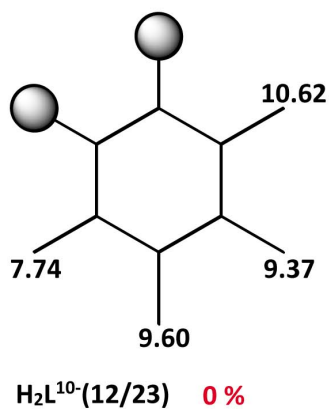
L<sup>12-</sup>

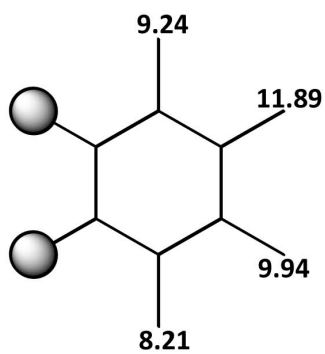


HL<sup>11-</sup>

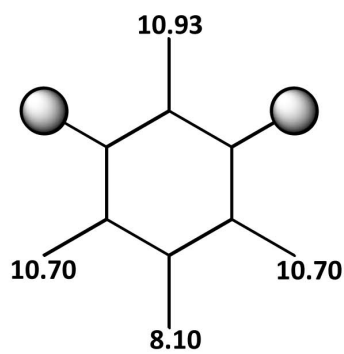


H<sub>2</sub>L<sup>10-</sup>

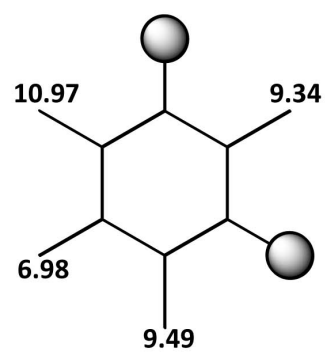




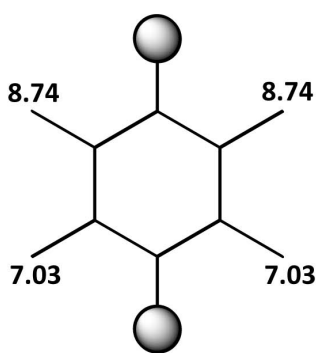
$H_2L^{10-}(16/34)$  **1.2 %**



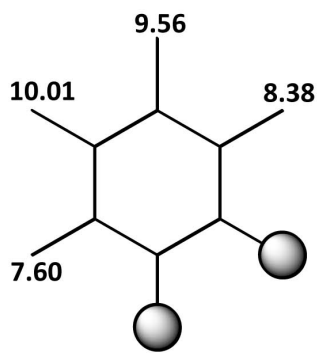
$H_2L^{10-}(13)$  **0 %**



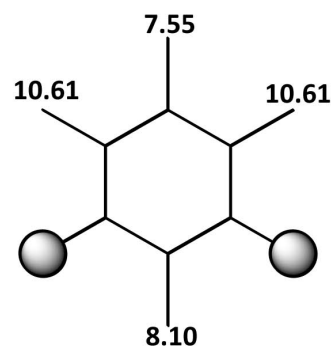
$H_2L^{10-}(24/26)$  **5.4 %**



$H_2L^{10-}(25)$  **47 %**

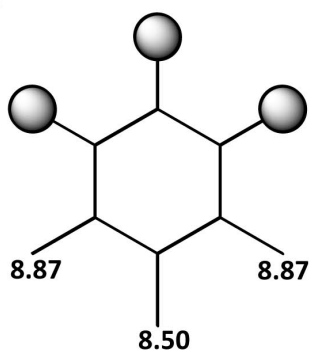


$H_2L^{10-}(45/56)$  **0 %**

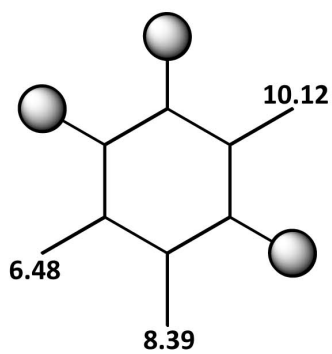


$H_2L^{10-}(46)$  **40 %**

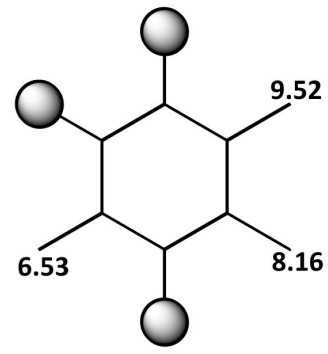
$H_3L^{9-}$



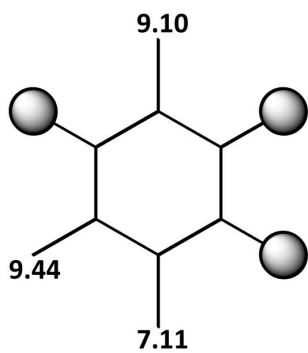
$H_3L^{9-}(123)$  **19.4 %**



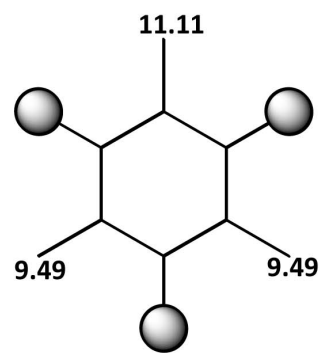
$H_3L^{9-}(124/236)$  **0 %**



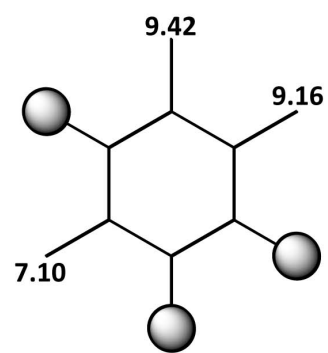
$H_3L^{9-}(125/235)$  **0 %**



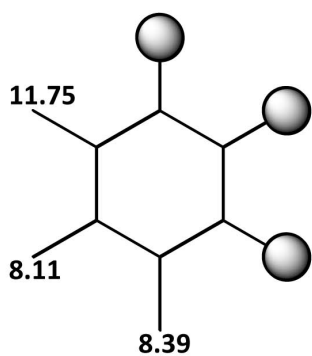
$H_3L^{9-}(134/136)$  **22.8 %**



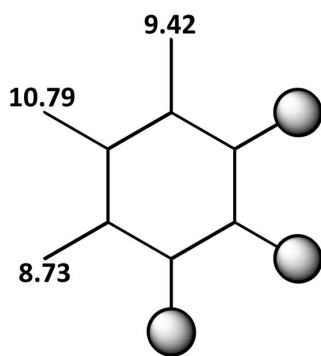
$H_3L^{9-}(135)$  **11 %**



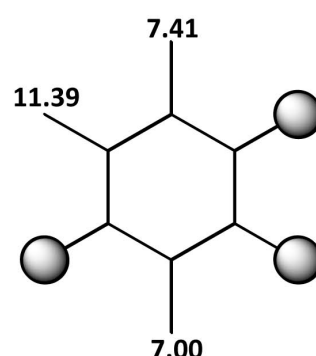
$H_3L^{9-}(145/356)$  **0 %**



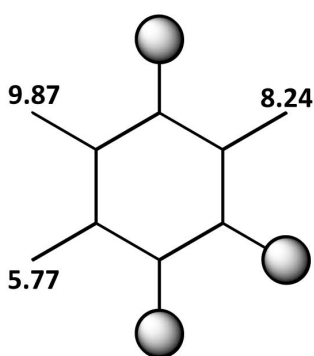
$H_3L^9-(234/126)$  0 %



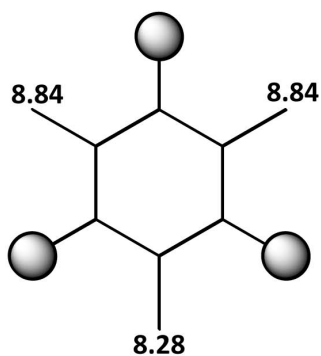
$H_3L^9-(345/156)$  0 %



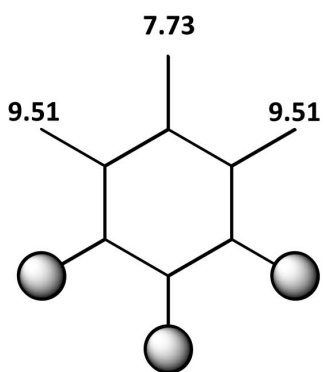
$H_3L^9-(346/146)$  0 %



$H_3L^9-(245/256)$  0 %

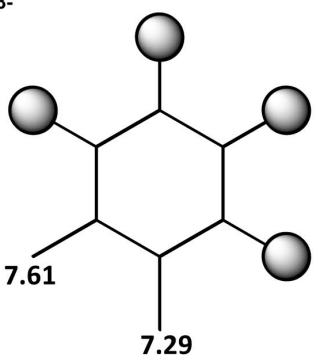


$H_3L^9-(246)$  46.6 %

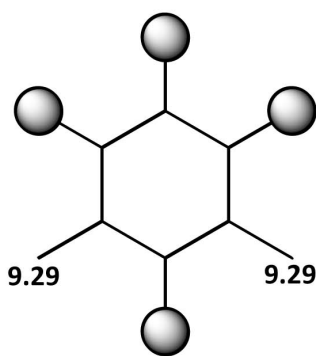


$H_3L^9-(456)$  0 %

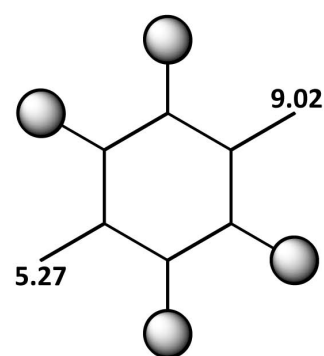
-----  
 $H_4L^{8-}$



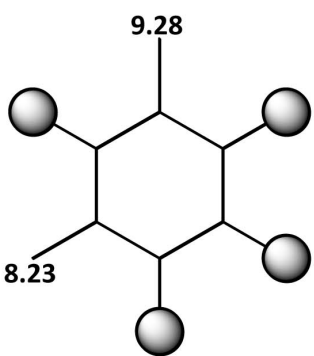
$H_4L^{8-}-(1234/1236)$  38.8 %



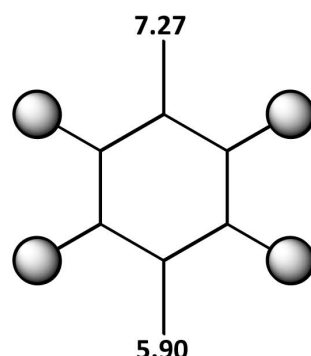
$H_4L^{8-}-(1235)$  0 %



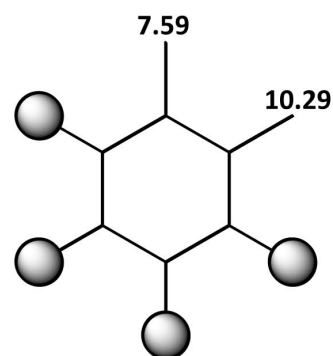
$H_4L^{8-}-(1245/2356)$  0 %



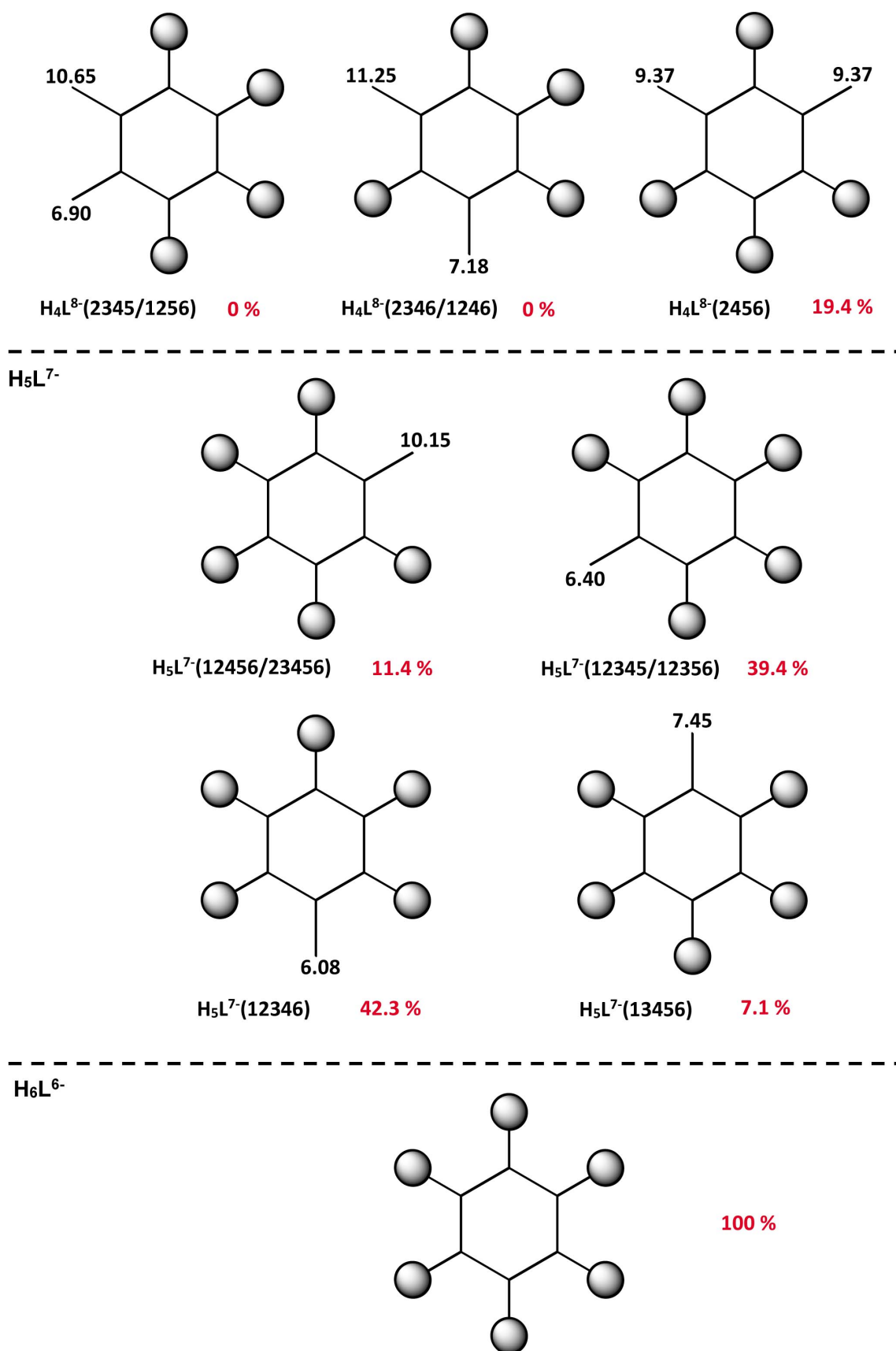
$H_4L^{8-}-(1345/1356)$  0 %



$H_4L^{8-}-(1346)$  41.7 %



$H_4L^{8-}-(1456/3456)$  0 %



Scheme S1. Macro and microstates of InsP<sub>6</sub> upon protonation. The logarithm of the microscopic protonation constants are shown for every deprotonated site, while the grey circles indicate the sites already protonated. The abundance of all the microstates within each macrostate are also listed.

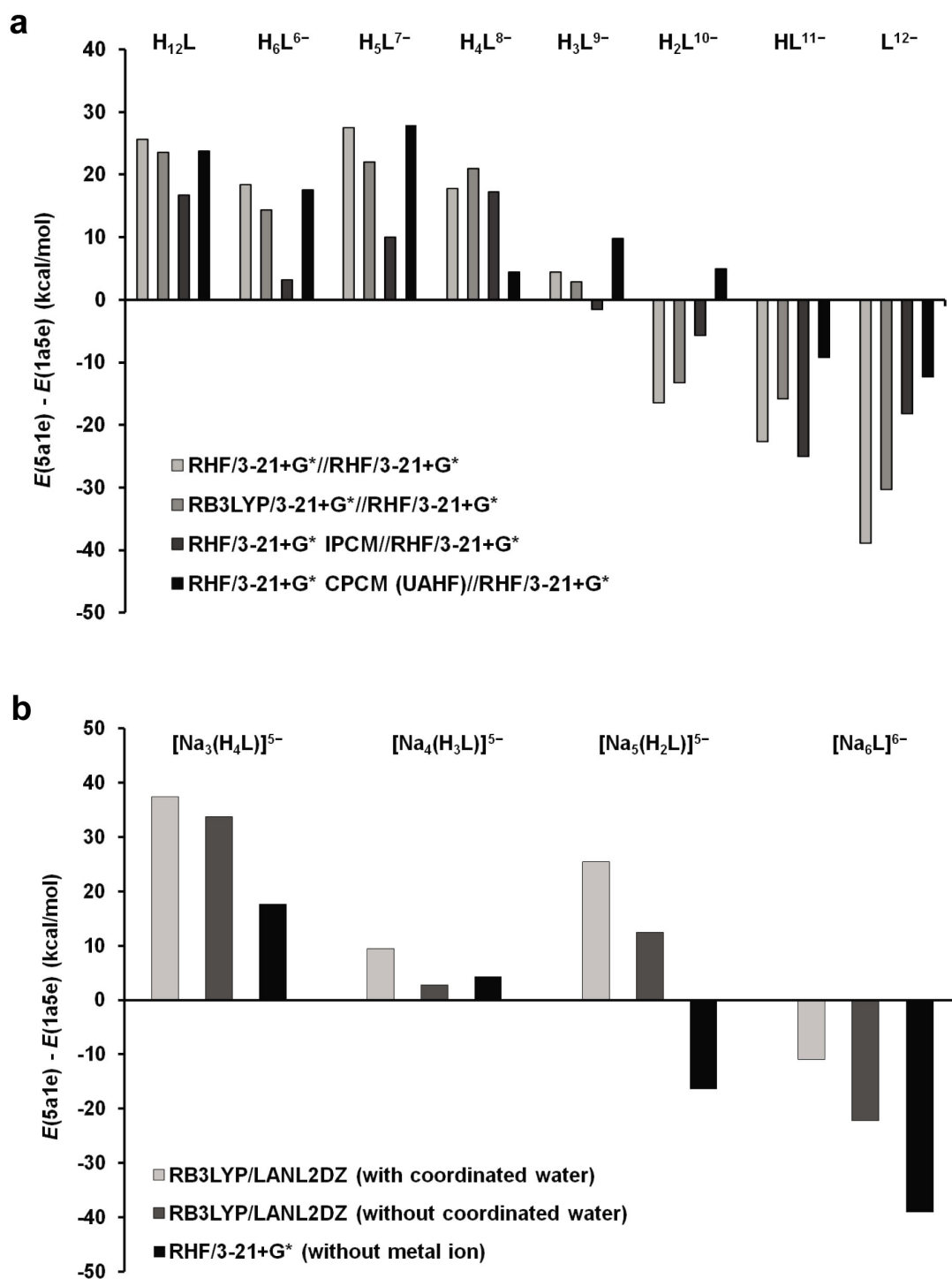
### *pH-dependant $\text{InsP}_6$ conformational change*

We analyzed the energy difference between 5a1e and 1a5e  $\text{InsP}_6$  conformers,  $\Delta E$ , as the successive species become more protonated (Figure S1a). In gas phase, the most deprotonated species ( $\text{L}^{12-}$ ,  $\text{HL}^{11-}$  and  $\text{H}_2\text{L}^{10-}$ ) have a preference for the 5a1e conformation, whereas the species with a medium to high degree of protonation (from  $\text{H}_3\text{L}^9$  to  $\text{H}_{12}\text{L}$ ) find 1a5e as the most stable state.

The average separation of the phosphorus atoms ( $X_{\text{P-P}}$ , Table 2) is always greater for 5a1e conformation, so the ionisable groups are more distant to one another when all are arranged in axial position. This effect is expected to be significant only when the ligand is highly deprotonated, making the 5a1e state preferred for  $\text{L}^{12-}$ ,  $\text{HL}^{11-}$  and  $\text{H}_2\text{L}^{10-}$  in gas phase. As the ligand becomes more protonated, phosphate groups begin to interact to one another through the formation of multiple hydrogen bonds (Figure 4). According to Table 2, the number ( $n$ ) and average distance ( $X_{\text{O-H}}$ ) of the intramolecular hydrogen bonds show that 1a5e conformation is slightly more effective to establish more and stronger H-bonds. Although, this factor does not seem to explain the observed conformational change, the establishment of a net of intramolecular H-bonds leads to the approach of the negatively charged groups, causing some tension in the carbon ring. As it is deduced from the average deviation of the dihedral angles formed by the axial groups ( $\Delta\theta_{\text{axial-axial}}$ ), the deformation of the chair is more pronounced for the 5a1e state, for the establishment of strong intramolecular hydrogen bonds between axial groups require a great structural alteration. Since this phenomenon becomes increasingly important with the decrease in pH, 1a5e conformation results more stable for protonated species, allowing a good phosphate- $\text{H}^+$ -phosphate interaction, with a minimum structural deformation.

The species  $\text{H}_4\text{L}^{8-}$  deserves a special comment. Unlike what occurs with the species  $\text{H}_3\text{L}^9$ , where the protons alternately neutralize the charge of a pair of phosphates, the addition of a fourth proton implies that at least two of these groups must now share two  $\text{H}^+$  by H-bonds. This structural requirement seems to be not easy to satisfy, as the phosphate groups, still highly charged, repel each other significantly. In consequence, even though both conformations suffer similar structural tension, only 1a5e state provides a spatial arrangement of the ionisable groups which results in shorter intramolecular hydrogen bonds.

Regarding the contribution of the solvent, for the highly charged phytate species the relaxing effect given by the geometry optimization in the presence of a dielectric may be not negligible. In spite of this, the gas phase geometries presented in this report are suitable representations of the structures in solution (they are in agreement with the experimental NMR data), and also the relaxing effect is partially cancelled in the  $\Delta E$  values.  $\Delta E$  values in water, determined by two different methods, IPCM and CPCM, are summarized in Figure S1a. In both methods, the solvation process is emulated by means of placing the species inside a cavity made of a dielectric material, as it is shown for  $\text{L}^{12-}$  in Figure S2.



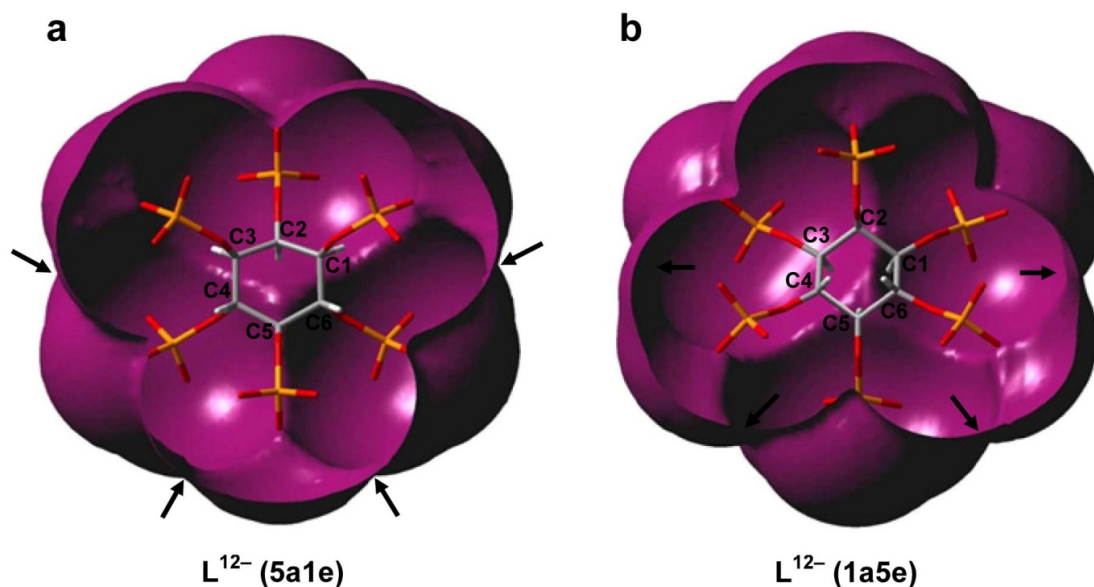


Figure S2.  $L^{12-}$  species inside the IPCM solvent cavity for 5a1e (a) and 1a5e (b) conformations (isodensity value =  $1 \times 10^{-5}$  e/bohr<sup>3</sup>). The arrows indicate the slight exclusion of the dielectric during the 5a1e-1a5e conformational change. Color code: C (grey), H (white), O (red), P (orange).

For all the protonated  $InsP_6$  forms, there are two main factors that modulate the relative stability of each conformer. First, it is energetically less expensive to approach two charged phosphate groups in the presence of a dielectric, favouring the 5a1e $\rightarrow$ 1a5e transition in solution. Secondly, according to Figure S2 the dielectric solvent is slightly excluded from the inter-phosphate space in 1a5e conformation, leading to a decrease in the aqueous stability of the equatorial state and somewhat counteracting the effect of the first factor.

IPCM and CPCM results follow the gas phase tendency. The relative stability of the conformers seems not to be altered by the hydration of the species. Nevertheless, as we found for  $Ins(1,3,4,5,6)P_5$ <sup>7</sup>, the  $InsP_6$ -water interaction would be critical for setting the pH range in which the conformational change occurs. CPCM results behave less erratically and are in line with our experimental data. Unlike in gas phase, where the transition is activated by the  $H_3L^9 - H_2L^{10}$  transformation, in the presence of water this process would be restricted to the second protonation of the ligand (see Figure S1a).

$M^+-InsP_6$  systems

The  $^{31}P$  NMR spectra registered for  $InsP_6$  in the presence of  $Na^+$  (a) and  $K^+$  (b) are shown in Figure S3.

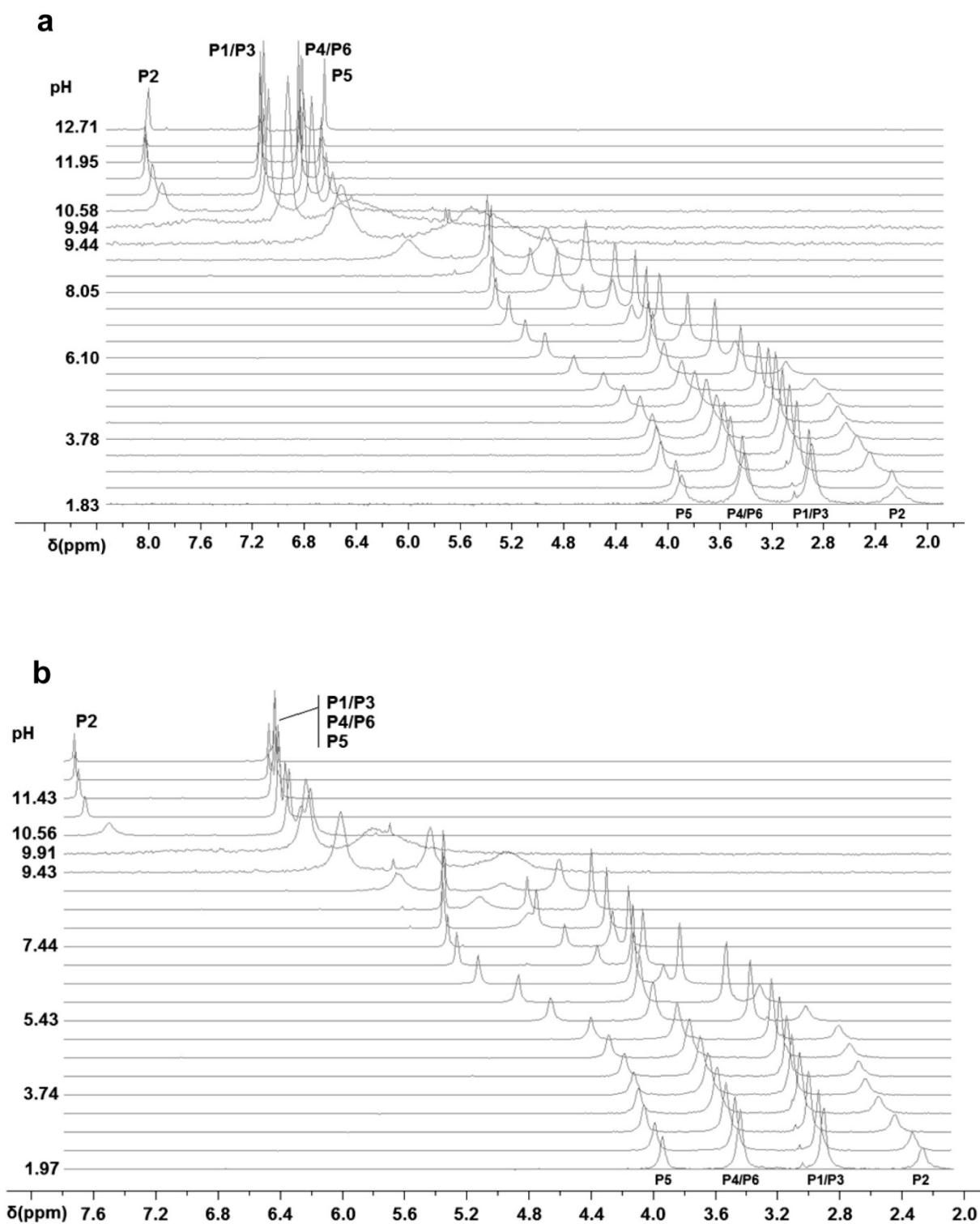


Figure S3.  $^{31}P$  NMR spectra for  $InsP_6$  as a function of pH ( $I = 0.15$  M,  $T = 37.0$  °C). (a)  $[InsP_6] = 5.02$  mM,  $[Na^+] = 152.5$  mM; (b)  $[InsP_6] = 5.15$  mM,  $[K^+] = 150.8$  mM.

The calculated individual chemical shifts for the detected  $\text{Na}^+ - \text{InsP}_6$  species are listed in Table S2. For  $[\text{Na}_6\text{L}]^{6-}$ , the  $\text{Na}^+$  cations seem to be linked to more than one phosphate group (Figures 6a and 6e) making the respective  $\Delta\delta_c$  values all different to one another. The 5a1e conformation of the ligand results to be more consistent with the calculated individual chemical shifts for this species (Table S2). In detail, P1/P3 and P4/P6 groups are the most involved in linking the sodium cations, through three or four oxygen atoms (highest  $\Delta\delta_c$ ). P5, however, binds the cations only as a bidentate group, being less affected. P2 is surrounded by three  $\text{Na}^+$  ions, but the spatial arrangement of the atoms make the average P-M<sup>+</sup> distance 0.2 Å larger, leading to the lowest  $\Delta\delta_c$  value (Table S2).

When the pH is lowered, a concerted sequence of protonation and metal dissociation processes becomes operative. The protonation of the ligand starts in positions 2 and 5 (see  $\Delta\delta_p$  in Table S2), giving rise to a significant structural change that ends up in the loss of one  $\text{Na}^+$  and leads to the formation of  $[\text{Na}_5(\text{H}_2\text{L})]^{5-}$ . The phosphates at C1/C3 and C4/C6 are the most affected by the complexation scheme, while P5 is probably linked to no more than one  $\text{Na}^+$ . Besides, according to the  $\Delta\delta_p$  for P1/P3 and P4/P6 groups, it is feasible that the former is only surrounded by metal ions, while the latter is sharing a proton with P5. This information raise an interesting aspect: only the modelled 1a5e state of  $\text{InsP}_6$  allows for an effective H-bond interaction between P4/P6 and P5, giving a structural explanation for the  $^{31}\text{P}$  NMR results (compare Figures 6b and 6f). This suggest a 5a1e  $\rightarrow$  1a5e conformational change, experimentally evidenced by the broadening of the NMR signals in the pH range 9.4 - 10.5 (Figure S3a), where both complexes  $[\text{Na}_5(\text{H}_2\text{L})]^{5-}$  and  $[\text{Na}_6\text{L}]^{6-}$  are predicted to coexist (Figure 3b).

At this point, it is worth analysing the behaviour of the P2 signal upon complexation. P2 is linked to one  $\text{Na}^+$  ion but, strikingly, its  $\Delta\delta_c$  is almost as high as those for P1/P3 and P4/P6. We propose two main mechanisms for this phenomenon. On the one hand, the equatorial hydrogen attached to C2 points directly to Na1 (C2-Na1 distance = 2.3 Å), producing a C2-H  $\cdots$  Na1 repulsion and in turn a change in the P2 environment (Figure 6b). As it can be seen from the  $\Delta\delta_c$  for P2 (Table S2), this effect remains in the 1a5e  $[\text{Na}_4(\text{H}_3\text{L})]^{5-}$  (Figure 6c), but disappear for 1a5e  $[\text{Na}_3(\text{H}_4\text{L})]^{5-}$  (Figure 6d), where Na1 is released to the solution. On the other hand, under the dynamics of the solution, Na5 ion is highly probable to interact with P2 (Figure 6b), contributing positively to the respective  $\Delta\delta_c$  value. In fact, the same through-space interaction is predicted for  $[\text{Na}_4(\text{H}_3\text{L})]^{5-}$  species (Figure 6c).

From now on, the structure of the other two complexes can be rationalized through a process of  $\text{H}^+ - \text{Na}^+$  interchange on the ligand, without the consideration of any conformational change whatsoever. The third incoming proton displaces one  $\text{Na}^+$  attached to P1/P3 and P4/P6, making their  $\Delta\delta_p$  values lower ( $[\text{Na}_4(\text{H}_3\text{L})]^{5-}$ , Figure 6c). As P2 is linked to P1/P3 via a strong H-bond, its signal is also affected. P5, however, seems not to be significantly affected in this process. The  $\Delta\delta_c$  are lower for P1/P3, since the protonation partially neutralizes the binding of one Na cation. Actually, the most abundant triprotonated microspecies of the ligand does not contain a protonated P1/P3 group:  $\text{H}_3\text{L}^{9-}$ (246). The fourth protonation step is accompanied by the loss of one  $\text{Na}^+$  cation previously bound to P2 and P1/P3. This leads to negative  $\Delta\delta_p$  and lower  $\Delta\delta_c$  values for these two phosphate groups. Both, P4/P6 and P5, are only slightly affected (Figure 6d).

In Table S2, the calculated individual chemical shifts for the  $K^+$ -Ins $P_6$  species are shown. An interesting aspect that first arises is the discrepancy between  $\Delta\delta_c$  for  $[Na_6L]^{6-}$  and  $[K_6L]^{6-}$  species, indicating that P1/P3 group is less involved in the complexation of  $K^+$  than of  $Na^+$ . This phenomenon is also evident in the difference between the  $^{31}P$  NMR spectra for both  $M^+$ -Ins $P_6$  systems at pH > 11, where  $[Na_6L]^{6-}$  and  $[K_6L]^{6-}$  are the predominant forms of phytate (Figures S3a and b and Figures 3b and c).

As it is deduced from the computational results for both species (Figure S4), the  $K^+$  ions are bulkier and as a consequence tend to repel one another in a greater extent, being their positions shifted towards the P4-P5-P6 side, and leaving P1, P2 and P3 groups less implicated in the coordination scheme.

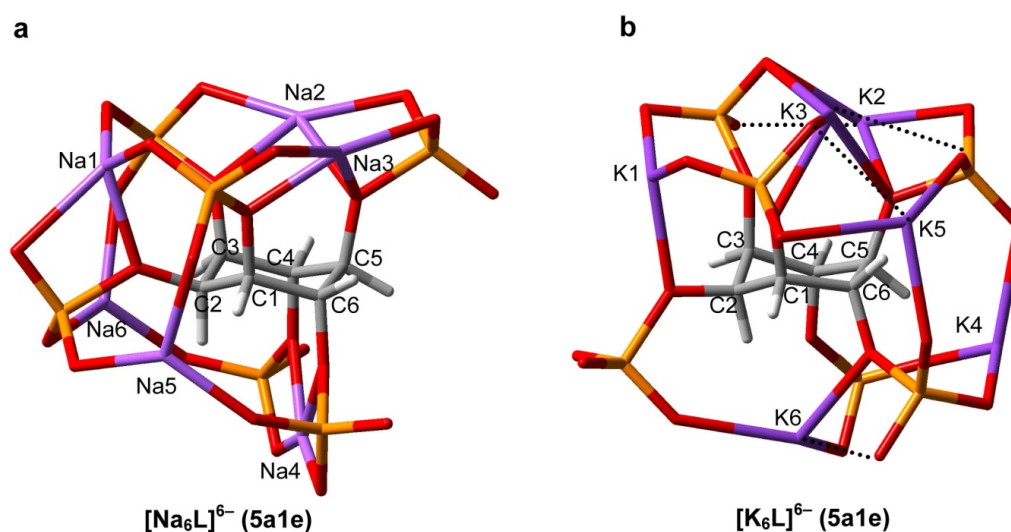


Figure S4. RB3LYP/LANL2DZ geometries for the 5a1e conformation of  $[Na_6L]^{6-}$  (a) and  $[K_6L]^{6-}$  (b) species. The weaker metal-ligand bonds are depicted as dotted lines. Color code: C (grey), H (white), O (red), P (orange), Na (violet).

The next complex species,  $[K_5(H_2L)]^{5-}$ , is produced by the loss of one  $K^+$  cation, which triggers the entrance of two protons. Even though all the phosphate groups are somewhat involved in the coordination of the  $K^+$  ions, they are likely to be linked mainly by P4/P6 and P1/P3. The  $\Delta\delta_p$  values point to P2 and P5 being protonated, although the latter seems to share its proton with P4/P6. The fact that P5 and P4/P6 are able to do this is an indication of a ligand conformational change, operative between  $[K_6L]^{6-}$  (5a1e) and  $[K_5(H_2L)]^{5-}$  (1a5e), in agreement with the broadening of the NMR spectra in the pH range 9.4 - 10.5 (Figure S3b), where both species are expected to predominate (Figure 3c).

According to the  $\Delta\delta_p$  values, it seems possible that in the process  $[K_5(H_2L)]^{5-} \rightarrow [K_4(H_3L)]^{5-}$  the  $K^+$ - $H^+$  exchange takes place between P1/P3 and P4/P6 groups. This would be consistent with a cationic rearrangement over the ligand, in which P1/P3 and P2 become less protonated and more involved in the metal complexation pattern (high  $\Delta\delta_c$  values). Finally, the loss of the third  $K^+$  lead to the formation of  $[K_3(H_4L)]^{5-}$ , and another  $H^+$  occupy the inter-phosphate space. In this complex P1/P3 and P2 share the new proton, while P4/P6 is concerned the most in the coordination of the metal ions (Table S2).

### *Na<sup>+</sup>-mediated conformational change*

In highly basic media, the phytate adopts the 5a1e conformation, for it is essential to minimize the substantial phosphate-phosphate repulsion. This effect is capable of deforming the inositol ring to a certain extent, giving rise to high  $\Delta\theta_{\text{axial-axial}}$  values. Interestingly, the complexation of six sodium cations relieves this tension (low  $\Delta\theta_{\text{axial-axial}}$ ), although this phenomenon is more pronounced for the 1a5e state of the ligand, because is the most sterically and electrostatically hindered. As a consequence, in the presence of sodium ions the  $\Delta E$  values in Figure S1b increase with respect to those for the ligand, yet this effect is not big enough to invert the stability of the conformations in the  $L^{12-} \rightarrow [Na_6L]^{6-}$  process. The axial disposition of the phosphate is still the preferred state: it has a higher value of  $X_{P-P}$ , allowing the phosphate groups to be farther to one another.

It is worth noticing that none monoprotinated species were detected under our experimental conditions. It seems feasible that the income of the first proton catalyzes the entrance of the second and the loss of one Na<sup>+</sup> ion, possibly through an important structural change. According to the values for  $[Na_5(H_2L)]^{5-}$  in Table 2, this phenomenon is so radical that ends up in a conformational transition, where the 1a5e state is stabilized. In fact, is the equatorial conformation which enables the formation of stronger H-bonds, with a minimum constraint imposed on the carbon ring (see Figures 6b and 6f). With the third protonation step, the establishment of strong hydrogen bonds become really important to stabilize the species. Thus, both conformations form three strong intramolecular H-bonds, yet the 5a1e form is still largely tensioned (higher value of  $\Delta\theta_{\text{axial-axial}}$ ). The same happens with the entrance of the fourth proton, though in this case the 1a5e disposition achieves stronger intramolecular H-bonds, with a minimum structural distortion. All this data are in line with the NMR data, reaffirming the 1a5e state as the most stable conformation under pH = 10.

Finally, according to the  $\Delta E$  values in Figure S1b, it can be seen that the inclusion of the solvent moderately favours the equatorial state. Looking at the structures in Figure 6, in the 1a5e conformation the Na<sup>+</sup>-H<sub>2</sub>O affinity tends to be lower than in the 5a1e state, leaving the cations less exposed to the solution and increasing the Na<sup>+</sup>-phosphate interaction energy.

$M^{2+}$ - $InsP_6$  systems

The  $^{31}P$  NMR spectra for an equimolar solution of  $InsP_6$  and  $Mg^{2+}$  (a) or  $Ca^{2+}$  (b) are shown in Figure S5.

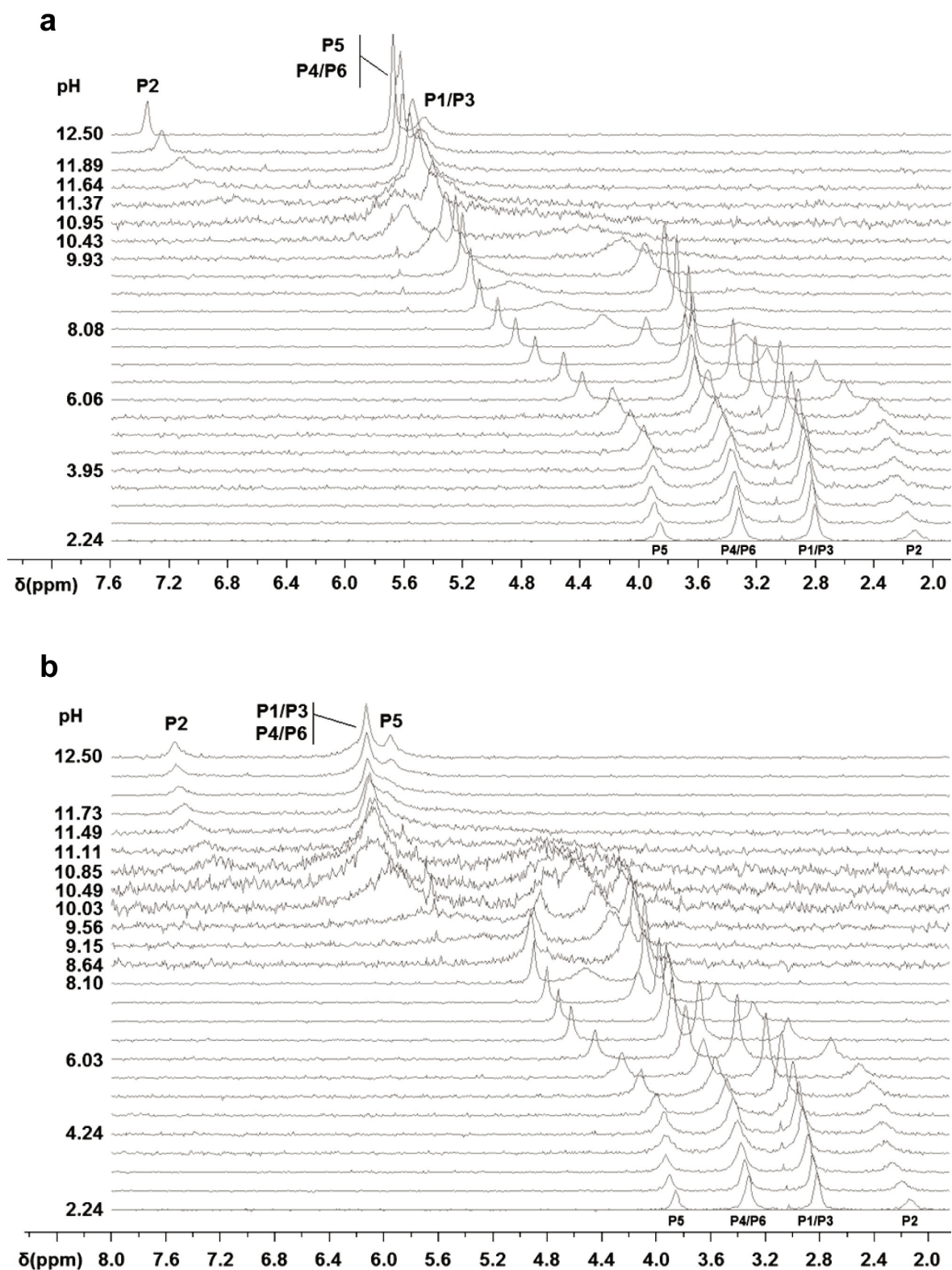


Figure S5.  $^{31}P$  NMR spectra for  $InsP_6$  as a function of pH ( $I = 0.15$  M,  $T = 37.0$  °C). (a)  $[InsP_6] = 1.99$  mM,  $[Mg^{2+}] = 1.99$  mM; (b)  $[InsP_6] = 2.05$  mM,  $[Ca^{2+}] = 2.03$  mM.

Table S2 lists the calculated individual chemical shifts for the  $M^{2+}$ -Ins $P_6$  species. According to previous reports, the addition of a divalent metal ion causes the ligand  $^{31}\text{P}$  chemical shifts to change positively or negatively, depending on the contribution of two main factors: a) a downfield effect brought about by the lost of protons and b) an upfield effect originated by the  $M^{2+}$  complexation processes<sup>8</sup>. With this in mind, we could monitor the position of each one of the  $\text{H}^+$  and  $M^{2+}$  on all the metal species detected. The results are summarized in Figure 9.

The  $\text{Mg}^{2+}$  and  $\text{H}^+$  cations in  $[\text{Mg}(\text{HL})]^{9-}$  are expected to be bound to P1/P3 and P5 respectively (lower  $\Delta\delta_c$  values, being even negative for P1/P3). This protonation and complexation scheme can only be supported by the 5a1e state of phytate, in which both phosphate groups are spatially closer (Figure 9a). It is worth mentioning that  $\Delta\delta_c$  is unusually high for P2 and P4/P6, although this could be explained by a protonic rearrangement from  $\text{HL}^{11-}$  to  $[\text{Mg}(\text{HL})]^{9-}$ ; the  $\text{H}^+$  ion migrates from P2-P4/P6 space to P1/P3, causing this downfield effect. When one extra proton is added,  $\Delta\delta_p$  changes substantially. The most affected groups are P2, P4/P6 and P5, whereas P1/P3 has an oddly high  $\Delta\delta_p$  value. This phenomenon can be supported by an internal reorganization of the cations, possibly motivated by a conformational flip of the ligand that permits the groups on C2, C4/C6 and C5 to participate actively in the coordination and protonation scheme. The low  $\Delta\delta_c$  values for  $[\text{Mg}(\text{H}_2\text{L})]^{8-}$  agree with these facts, indicating that the complex and the  $\text{H}_2\text{L}^{10-}$  species would share the same conformational state (1a5e). According to the species distribution diagram (Figure 8a), the  $[\text{Mg}(\text{HL})]^{9-} \rightarrow [\text{Mg}(\text{H}_2\text{L})]^{8-}$  process is operative between  $\text{pH} = 10$  and 12, where the expected broadening of the signals comes into sight in the NMR spectra (Figure S5a). Considering the 1a5e conformation, it seems logical that  $[\text{Mg}(\text{H}_2\text{L})]^{8-}$  could have the  $\text{Mg}^{2+}$  being coordinated by P2, P1/P3 and P4/P6, while both protons would be linked to P5 and P4/P6. In this regard, the  $[\text{Mg}(\text{HL})]^{9-} \rightarrow [\text{Mg}(\text{H}_2\text{L})]^{8-}$  process would mostly affect P2 and P4/P6 (lower  $\Delta\delta_p$  values) whereas P1/P3 ends up deprotonated and farther from the  $\text{Mg}^{2+}$  ion (higher  $\Delta\delta_p$  value). Additionally, in the  $\text{H}_2\text{L}^{10-} \rightarrow [\text{Mg}(\text{H}_2\text{L})]^{8-}$  step, the P4/P6 signal would be the considerably influenced, for this group is not only protonated but also participates in the magnesium complexation. In the same reaction, P5 has now two protons ( $\Delta\delta_c < 0$ ), while P2 and P1/3 are only slightly affected: the  $\text{Mg}^{2+}$  ion displaces a proton formerly located between this two phosphate groups, cancelling the effect.

For the rest of the complexes, the 1a5e conformation seems to be the preferred one (Figure 9a). This can be deduced from the calculation of  $\Delta\delta_L$ , the variation of the chemical shifts in the process  $\text{L}^{12-}$  (5a1e)  $\rightarrow [\text{M}(\text{H}_x\text{L})]^{(10-x)-}$  (Table S4). The  $\Delta\delta_L$  values are progressively more negative from  $[\text{Mg}(\text{H}_3\text{L})]^{7-}$  to  $[\text{Mg}(\text{H}_6\text{L})]^{4-}$ , giving support to the 5a1e - 1a5e transition for all of them.

The third incoming proton would be situated on P2-P1/P3 space (low  $\Delta\delta_p$  values, Figure 9a), making the  $\text{Mg}^{2+}$  ion to migrate towards P4/P6 group ( $\Delta\delta_p < 0$ ). Starting from  $\text{H}_3\text{L}^{9-}$ ,  $\Delta\delta_c$  points to P2 as the most affected by the complexation, because it remains bound to the metal ion and also retains one proton in its surroundings. In addition, the  $\text{H}^+$  ions tend to be shifted to P5, getting away from P1/P3.

From this species to  $[\text{Mg}(\text{H}_6\text{L})]^{4-}$ , the latter coordination scheme is preserved. In fact, the  $\Delta\delta_L$  values show that P2, P4/P6 and P1/P3 are part of the magnesium coordination sphere, while P5 bears the migration of protons (Table S4).

Cation	Species	$\Delta\delta_L$ (ppm)			
		P1/P3	P2	P4/P6	P5
$Mg^{2+}$	$[Mg(HL)]^9$	-0.637	0.112	0.184	-0.165
	$[Mg(H_2L)]^8$	0.172	-2.370	-1.220	-0.596
	$[Mg(H_3L)]^7$	-0.794	-4.215	-1.635	-0.548
	$[Mg(H_4L)]^6$	-2.018	-4.007	-2.002	-0.977
	$[Mg(H_5L)]^5$	-2.889	-4.851	-1.943	-1.503
	$[Mg(H_6L)]^4$	-3.201	-5.199	-2.274	-1.995
$Ca^{2+}$	$[CaL]^{10}$	0.181	0.226	0.603	0.137
	$[Ca(HL)]^9$	0.081	0.175	-1.584	0.816
	$[Ca(H_2L)]^8$	0.396	-3.960	-1.199	-1.800
	$[Ca(H_3L)]^7$	-0.676	-2.674	-1.370	-0.765
	$[Ca(H_4L)]^6$	-1.669	-3.742	-1.511	-1.008
	$[Ca(H_5L)]^5$	-2.657	-4.797	-1.835	-1.447
	$[Ca(H_6L)]^4$	-3.237	-5.251	-2.339	-2.087

Table S4. Change in the  $^{31}P$  NMR chemical shifts for  $Mg^{2+}$ - $InsP_6$  and  $Ca^{2+}$ - $InsP_6$  systems (HypNMR software <sup>1</sup>) due only to the  $L^{12-} \rightarrow [M(H_xL)]^{(10-x)-}$  process ( $I = 0.15$  M,  $T = 37.0$  °C).

$[Mg(H_4L)]^6$  is produced by one more proton being linked to P1/P3 and P4/P6 (negative  $\Delta\delta_p$  values, Figure 9a). The P5 environment is somehow influenced through the space by the H-bond network. All the  $\Delta\delta_c$  values are substantial, giving the idea that all the phosphate groups are altered during the  $H_4L^{10-} \rightarrow [Mg(H_4L)]^8$  step. This can be rationalized taking into account the predominant microstates for the tetraprotonated form of phytate:  $H_4L^{10-}(1234/1236)$  and  $H_4L^{10-}(1346)$ . P2 is clearly the most affected group, for it retains its proton and it is "pulled back" to bind to the  $Mg^{2+}$  ion ( $\Delta\delta_c < 0$ ). P4/P6 and P5 signals are also changed. In the complexation process the first one binds the  $Mg^{2+}$  ion, while the second is surrounded by two protons. P1/P3 is only slightly influenced. This group experiments an  $Mg^{2+}$ - $H^+$  exchange that partially counter the change in  $\delta$ .

The structural analysis for the next two Mg complexes is not straightforward. All the inter-phosphate spaces have been filled with cations, and the incoming protons are bound to be linked to an ionizable group already associated to the  $Mg^{2+}$ - $H^+$ -phosphate bond network. This explains why all the signals are deeply modulated by the fifth and sixth protonation steps. Despite this situation, it would be feasible that the fifth incoming proton in  $[Mg(H_5L)]^5$  could be bound to P2 and P1/P3 groups, in some way affecting P5 through the net of H-bonds (lower  $\Delta\delta_p$ ).

We performed the same structural assessment for the calcium containing system. Taking into consideration the high positive  $\Delta\delta_L$  values from Table S4, the totally deprotonated form of  $InsP_6$  strongly interacts with  $Ca^{2+}$  ion to give the complex  $[CaL]^{10-}$ , where P1/P3 and P5 would be directly connected to the metal ion (lower  $\Delta\delta_L$ , Figure 9b). This is consistent with a 5a1e conformation of the

ligand, which also explains the great difference in the P4/P6 environment with respect to the rest of the ionizable groups (notably high  $\Delta\delta_L$  value). This complex species is protonated on P4/P6, according to its  $\Delta\delta_p$  value. This would reinforce the 5a1e state, compelling the calcium ion to be kept above the ring. However, due to repulsion, the  $\text{Ca}^{2+}$  cation tend to move away as far as possible from the incoming  $\text{H}^+$ , migrating from P5 towards the P1/P3-P2 space ( $\Delta\delta_p < 0$  for P2 and P1/P3;  $\Delta\delta_p > 0$  for P5). The  $\Delta\delta_c$  values agree with this protonation and complexation scheme: P2 is deshielded (it is in part bound to  $\text{Ca}^{2+}$  but it completely lost a proton from  $\text{HL}^{11-}$ ), P4/P6 is shielded (it is protonated), P1/P3 is poorly affected (there is a calcium to proton exchange on it) and P5 is deshielded (it has a  $\text{Ca}^{2+}$  ion at a distance which partially attracts its electron density).

From  $[\text{Ca}(\text{H}_2\text{L})]^{8-}$  to  $[\text{Ca}(\text{H}_6\text{L})]^{4-}$  the  $\Delta\delta_L$  values are highly negative for P2, P4/P6 and P5 (Table S4). This is an indication of a possible conformational transition of the ligand. As a consequence, the broadening and noise of the NMR signals raise below  $\text{pH} = 11.5$ , where  $[\text{Ca}(\text{H}_2\text{L})]^{8-}$  becomes detectable (Figures S5b and 8b).  $\Delta\delta_p$  for this complex shows that P2 and P5 are protonated, while P2 would also be bound to the  $\text{Ca}^{2+}$  ion (highly negative  $\Delta\delta_p$ ; see Figure 9b). Probably, the spatial requirements given by the coordination scheme prevent the proton linked to P2 from being shared to P1/P3, making its  $\Delta\delta_p$  a positive value. For P4/P6 the deshielding effect is explained by the changes in its environment during the process  $[\text{Ca}(\text{HL})]^{9-} \rightarrow [\text{Ca}(\text{H}_2\text{L})]^{8-}$ : it starts to share with P5 the  $\text{H}^+$  which was formerly attached only to this group. Even though P4 (or P6) binds the calcium directly, this effect is countered to some extent by the deshielding effect caused by the distant metal ion over P6 (or P4). The  $\Delta\delta_c$  values are in line with this structure. The lowest  $\Delta\delta_c$  are those for P2 and P5, for both protons in  $[\text{Ca}(\text{H}_2\text{L})]^{8-}$  become restricted to positions 2 and 5, when in  $\text{H}_2\text{L}^{10-}$  were also situated in positions 4 and 6.

When  $[\text{Ca}(\text{H}_3\text{L})]^{7-}$  is produced from  $[\text{Ca}(\text{H}_2\text{L})]^{8-}$  an internal rearrangement of the protons is predicted (Figure 9b).  $\Delta\delta_p$  for P1/P3 and P2 are high and opposite in sign, which could be interpreted by a shift in the  $\text{H}^+$  that they share. A second proton could fill the P1/P3-P4/P6 space, as far away as possible from de metal cation (associated to P2-P1/P3-P4/P6). The last hydrogenion would be attached to P5 and P4/P6 (linked to the  $\text{Ca}^{2+}$  ion), making the P5 group closer to the calcium atom and explaining the increment in its  $\delta$ . The  $\Delta\delta_c$  are higher for P1/P3, because the union of calcium provokes a proton displacement in these groups in two of the most abundant microspecies of the ligand:  $\text{H}_3\text{L}(123)^{9-}$  and  $\text{H}_3\text{L}(134/136)^{9-}$ . Strikingly, P5 is the only group with a negative  $\Delta\delta_c$ . In fact, P5 is protonated only in the 11 % of  $\text{H}_3\text{L}^{9-}$ , while in  $[\text{Ca}(\text{H}_3\text{L})]^{7-}$  is predominantly associated with one  $\text{H}^+$ . The fourth protonation step is mediated by the protonation of P5-P4/P6 hole. It is likely that this phenomenon could trigger an internal relocation of the protons, and a migration of the metal ion towards the P1/P3-P2 space. This could give an explanation for the low  $\Delta\delta_p$  for P1/P3 and P2 (bound to  $\text{Ca}^{2+}$ ) and the small  $\Delta\delta_p$  for P4/P6 and P5 (through-space calcium-mediated deshielding effect). In support of this, P2 and P5 have the lowest  $\Delta\delta_c$ : the former binds calcium and the latter is surrounded now by two protons (deprotonated in the predominant tetraprotonated microspecies).

The fifth and sixth protonation are difficult to interpret.  $\Delta\delta_p$  and  $\Delta\delta_c$  are all negative figures, making the analysis an impossible task. Again, all the phosphate-phosphate spaces are filled with cations, and the incoming protons affect all the signals through the  $\text{Ca}^{2+}$ - $\text{H}^+$ -phosphate bond network.

The phytate  $^{31}\text{P}$  NMR spectra for different ligand and Mg concentrations are shown in Figure S6.

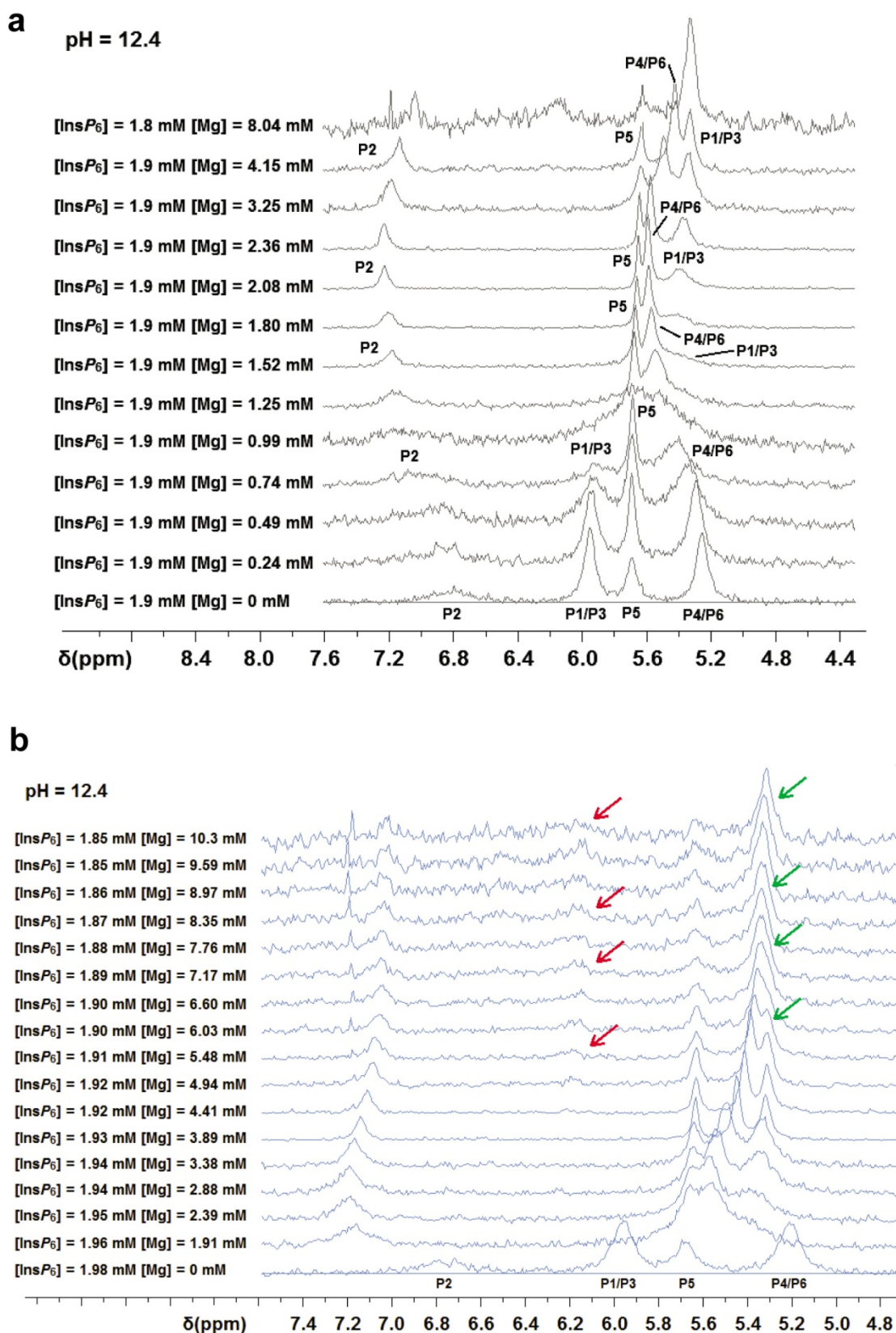


Figure S6. (a)  $^{31}\text{P}$  NMR spectra for InsP<sub>6</sub> as a function of the metal and ligand concentration ( $I = 0.15$  M  $\text{NMe}_4\text{Cl}$ ,  $T = 37.0$  °C, pH = 12.4). In (b), an extension of the same experiment is shown.

### References

- 1 C. Frassinetti, S. Ghelli, P. Gans, A. Sabatini, M. S. Moruzzi and A. Vacca, *Anal. Biochem.*, 1995, **231**, 374-382.
- 2 J. Torres, S. Domínguez, M. F. Cerdá, G. Obal, A. Mederos, R. F. Irvine, A. Díaz and C. Kremer, *J. Inorg. Biochem.*, 2005, **99**, 828-840.
- 3 J. Torres, N. Veiga, J. S. Gancheff, S. Domínguez, A. Mederos, M. Sundberg, A. Sánchez, J. Castiglioni, A. Díaz and C. Kremer, *J. Mol. Struct.*, 2008, **874**, 77-88.
- 4 C. Blum-Held, P. Bernard and B. Spiess, *J. Am. Chem. Soc.*, 2001, **123**, 3399-3400.
- 5 M. Borkovec and G. J. M. Koper, *Anal. Chem.*, 2000, **72**, 3272-3279.
- 6 N. Veiga, J. Torres, G. González, K. Gómez, D. Mansell, S. Freeman, S. Domínguez and C. Kremer, *J. Mol. Struct.*, 2011, **986**, 75-85.
- 7 N. Veiga, J. Torres, I. Macho, K. Gómez, H. Y. Godage, A. M. Riley, B. V. L. Potter, G. González and C. Kremer, *Dalton Transactions*, 2013, **42**, 6021-6032.
- 8 A. Bebot-Brigaud, G. Dange, N. Fauconnier and C. Gérard, *J. Inorg. Biochem.*, 1999, **75**, 71-78.